Journal of Building Engineering 87 (2024) 108968



Contents lists available at ScienceDirect

Journal of Building Engineering

journal homepage: www.elsevier.com/locate/jobe



# The effect of using seashells as cementitious bio-material and granite industrial waste as fine aggregate on mechanical and durability properties of green flowable sand concrete

Moussa Hadjadj [a], Mohamed Guendouz [a,b,*], Djamila Boukhelkhal [a,b]

[a] Laboratory of Materials and Environment (LME), University of Medea, Medea, 26000, Algeria
[b] Department of Civil Engineering, University of Medea, Medea, 26000, Algeria

ARTICLE INFO

*Keywords:*
Granite waste
Seashell powder
Flowable sand concrete
Mechanical properties
Durability

ABSTRACT

The present work is a study of the feasibility of using seashell powder (SSP) combined with industrial granite waste (GW) to develop a new green flowable sand concrete (FSC). The GW was used to replace the natural sand at levels of 0, 10, 20, 30, 40, and 50% by volume, and the SSP has been used to substitute the cement at levels of 5, 10, and 15% by weight. Slump flow and V-funnel flow time tests have been used to investigate the fresh properties of FSC mixtures. Compressive strength, modulus of elasticity, ultrasonic pulse velocity (UPV), water absorption, porosity, and acid attack tests were used to assess the mechanical and durability properties of hardened FSC mixtures. XRD, TGA, and SEM analyses were performed to evolve the microstructure of hardened FSC. The results showed a decrease in the fresh properties of FSC mixtures with the substitution of sand by GW. Nonetheless, the inclusion of SSP as filler mitigated this adverse effect, and all FSC mixes were subsequently discovered to be within the standard limits. The combined use of 50 vol % GW and 10 wt% SSP developed FSC with the greatest compressive strength (67 MPa), modulus of elasticity (40 GPa), and UPV (4175 m/s), as well as the lowest porosity (2.9%) and absorption (2.4%) at 90 days, compared to the control FSC. Moreover, using up to 10 wt% SSP with a fineness of 8000 $cm^2/g$ may enhance the durability of GW-based FSC against acid attack. Microstructural analyses indicated denser microstructure, stronger ITZ, and weaker porosity. The developed eco-friendly FSC effectively showed a decrease in production costs and carbon emissions, reducing the level of waste and protecting natural resources, which provides an emerging approach for its application in advanced green concretes for future work.

## 1. Introduction

In building construction, flowable sand concrete (FSC) has demonstrated a number of benefits, like pumpability, absence of segregation, ease of use, and implementation [1]. The composition of FSC (cement, filler, and sand) appears in their fresh state properties; it must be characterized by high deformability and filling ability without loss of stability [2]. These characteristics aid in making sure that constructions are resistant and durable, as well as economics [3]. FSC mix requires significant volumes of Portland cement and superplasticizers (SP) to meet these specifications [1], but significant amounts of Portland cement have negative environmental effects owing to $CO_2$ emissions, high manufacturing costs (manufacturing energy), and reduction of natural resources [4].

* Corresponding author. Laboratory of Materials and Environment (LME), University of Medea, Medea, 26000, Algeria.
*E-mail addresses:* guen12moh@gmail.com, guendouz.mohamed@univ-medea.dz (M. Guendouz).

https://doi.org/10.1016/j.jobe.2024.108968
Received 30 August 2023; Received in revised form 22 February 2024; Accepted 28 February 2024
Available online 6 March 2024
2352-7102/© 2024 Elsevier Ltd. All rights reserved.

The building industry is now investigating the use of waste and byproducts in construction to preserve more natural resources and reduce $CO_2$ emissions as a result of rising worries about the depletion of the planet's natural resources and global pollution [5–7]. The use of mineral admixtures as supplementary cementitious materials has helped concrete mixes perform in terms of compaction, mechanical, environmental and economic aspects [4].

Seashell wastes that amass in coastal locations can be processed, crushed and utilized as concrete components [8]. In general, seashells contain a lot of calcium (CaO) and therefore can be used as a cement replacement to improve the mechanical and durability properties of concrete due to the pozzolanic reaction that takes effect during cement hydration [9]. Around the world, 45,000 tons of trash seashells are generated annually, including mussel shells such as oyster shells, periwinkle shells, scallop shells, and cockleshells [10–14]. Numerous studies have investigated the use of seashell waste as a powder (SSP) in concrete manufacturing and demonstrated an enhancement of concrete performance with this waste [15–20]. Tayeh et al. [10] studied the effect of using seashell ash powder as cement replacement at levels of 5%, 10%, 15%, and 20%. The results show that adding 5% seashell powder to concrete improves its workability, compressive and tensile strength, and resistance to sulphate and alkali attacks. Seo et al. [21] examined the impact of adding 3%, 6%, 9%, and 12% of oyster shell powder as a cement weight substitute in mortar composition. The results showed an enhancement in the compressive strength and autogenous shrinkage qualities of the mortar with the addition of 3% oyster shell powder. Abdelouahed et al. [22] studied the use of seashells as cement substitutes with ratios of 5%, 10%, 15%, and 20%. The results indicated that the replacement of 5% cement with seashells caused an increase in the mechanical strength of the mortar at a young age and that the mortar based on 10% SSP showed the lowest chloride ion penetration. In another study, Rollakanti et al. [23] used 10, 20, and 30% seashell powder in place of cement and found that the compressive strength remained constant at 10% and subsequently fell as the proportion of seashell powder increased. Soltanzadeh et al. [24] looked at the effect of using up to 30% seashells as an addition to cement. The results indicated that seashell powder may be utilized as cement with improvement in durability and performance of concrete, as well as reducing manufacturing costs. Maglad et al. [25] investigated the effect of using 5, 10, 15, 20, 25, and 30% seashell ash as cement replacement on the properties of lightweight foamed concrete. The findings showed an increase in initial and final setting times, as well as a decrease in the spread and density of the fresh concrete. In addition, the replacement of cement with up to 15% seashell ash also enhanced the compressive, flexural, and splitting tensile strengths by 12.41%, 15.89%, and 17.95%, respectively, and performed better as pore filler than other replacement rates. Sangeetha et al. [26] studied the potential use of 5%, 10%, and 15% seashell powder as cement substitutes to produce eco-friendly concrete. It was found that there was an improvement of 30% in compressive strength at 90 days, and the optimal replacement rate is 5%.

On the other hand, massive amounts of solid waste are generated annually from the continual production of the stone industry's products, which is considered one of the most ecologically unfriendly practices [27]. Particularly granite (GW) which is then dumped in open landfills [28,29]. GW can be used in the construction field due to its availability and, most importantly, to its high-quality and good chemical and physical characteristics [30,31]. According to Karmegam et al. [32], granite particles are more resistant to heat, cold, moisture, stains, fractures, and scratches. Several researchers have discovered the potential of using granite waste in concrete manufacturing. Singh et al. [33] found an increase in compressive and flexural strength and a decrease in the permeability of concrete by substituting 25% of natural sand with granite cutting waste. Vijayalakshmi et al. [34] studied the impact of using GW as a partial substitute for river sand on the mechanical performance and durability of concrete. The results showed that up to 15% of GW can be used without negatively affecting these properties. Ghannam et al. [35] revealed a favorable effect on the mechanical properties of concrete by partially replacing river sand with GW. Cordeiro et al. [36] reported a negative effect on the rheological properties of concrete mixtures when using GW as a river sand substitute. However, adding more superplasticizer (SP) mitigated this effect. Binici and Aksogan [37] discovered that concrete made from granulated granite as fine aggregate has superior durability properties to those of conventional concrete. It has also been observed that the addition of fine granite aggregate provides a better condensed matrix, resulting in less permeable concrete. Nuaklong et al. [38] investigated the effect of replacing 25 and 50% of the natural river sand with granite waste on the properties of geopolymer concrete. It was found that increasing the proportion of GW in the mix resulted in an increased slump flow of concrete. Meanwhile, the early compressive strength improved when 50% of the natural sand was replaced with granite waste. In terms of sustainability, Jain et al. [39] found that, taking into account the specified economic and environmental cost factors, using up to 40% of GW in place of fine aggregates could be beneficial for the production of SCC.

The current study is part of the process of recycling and reusing waste in the construction industry, notably aggregates and cement, in an effort to decrease the extraction of aggregates and $CO_2$ emissions while extending the life of landfills currently in saturation, which is very advantageous from an ecological and financial standpoint. From the literature review, several studies have been conducted on the effect of the single use of SSP as cement and GW as a substitute for fine or coarse aggregate on the properties of ordinary concrete. However, the possibility of their use in a combined manner to simultaneously replace parts of cement and aggregate in ordinary and flowable sand concrete has not been investigated. This study was carried out to investigate the effect of the combined use of SSP as a cement addition and GW as a substitute for fine aggregate (natural sand) on the flow, the compressive strength, the ultrasonic pulse velocity, the modulus of elasticity, the porosity and water absorption, and the acid attack of FSC. To assess the microstructural characteristics of some FSC mixtures, scanning electron microscopy (SEM), X-ray diffraction (XRD) and thermogravimetric (TGA) analyses have also been performed.

## 2. Materials and methodology

### 2.1. Materials

#### 2.1.1. Cement, marble powder and seashell powder

For this investigation, all FSC mixtures were made using Ordinary Portland Cement (OPC) type CEMI 42.5 from the Mascara

Factory (Algeria), which complies with EN 197-1 [40]. The use of fillers is essential in the composition of flowable sand concrete [41]. Marble powder (MP), produced by crushing and grinding waste products of white marble tiles from marble stone sawing and polishing factories in Medea, Algeria, was used as filler in this study.

Seashell powder (SSP) is a marine by-product obtained from crushing the seashell waste that is rejected in the littorals. The seashell waste used in this study was obtained by recovering oysters collected from the El Kadouce Beach Sea (a site located in the capital of Algiers). After being immersed in water for 24 h, these shells were cleaned with a brush to remove all impurities and salt content and oven-dried for 4 h at 105 °C. The shells were then mechanically treated to enhance their fineness by utilizing the Los Angeles machine with 2000 crushing rotations to obtain a very fine powder with a Blaine-specific area (SSB) equal to 8000 $cm^2/g$. To better activate the calcium carbonate phases ($CaCO_3$) and decompose them to CaO, the SSP was heat-treated in an oven for 2 h at a temperature of 650 °C.

The visual appearance, chemical composition, and physical properties of cement, marble powder, and seashell powder are depicted in Fig. 1 and Table 1, respectively. The preparation process of the raw materials used in this study is presented in Fig. 2.

#### 2.1.2. Fin aggregates

Local siliceous sand from the Oued Souf quarry near Bouira city (south of Algeria), with a maximum diameter of 4.75 mm, was used as fine natural aggregate. Granite waste (GW) produced during the cutting and polishing activities of granite stone factories located in the Chrachria region of Medea, Algeria, was used as recycled fine aggregates. After their collection and crushing to transform into grains (Fig. 3), they were used to substitute natural sand in volumetric amounts of 10%, 20%, 30%, 40%, and 50% to manufacture FSC. The morphology and visual appearance, chemical composition, and physical properties of natural sand and GW sand are depicted in Fig. 3 and Table 2, respectively.

#### 2.1.3. Water and admixture

A high-water-reducing superplasticizer (based on polycarboxylate ether) named 'MEDAFLOW30' and manufactured by GRANITEX Company was used as a chemical admixture to achieve sufficient flowability in the fresh FSC mixture. It has a liquid form, a yellowish color, a specific gravity of 1.08 $g/cm^3$, a solids content of 30 wt%, a pH of 6.25, and a chlorine content of less than 1 g/L. The normal range of use of this superplasticizer, as fixed by the data sheet, is between 0.3 and 2% of the cement weight. Potable tap water from the civil engineering laboratory of the University of Medea with a PH between 6.5 and 8 in accordance with NF EN 1008 [42] was used to mix all the concrete mixture ingredients and store the test specimens.

### 2.2. Mix proportions

For the purpose of evaluating how the combination of SSP and GW affects the rheological, mechanical, and durability characteristics of FSC, nineteen mixtures were prepared and tested in this study, with an overall powder content of 602.79 $kg/m^3$ (Portland cement and fillers) and 1400 $kg/m^3$ total aggregate content, while keeping the water/powder (W/P) ratio at 0.44. The amount of superplasticizer was adjusted for each FSC mix to achieve satisfactory fluidity and viscosity, with a target desired slump flow diameter of 270 ± 10 mm according to EFNARC recommendations [43].

The control FSC mixture (without SSP or GW) was developed according to the method proposed by the Sablocrete project [41], with modifications made to the water/powder ratio (W/P) and the superplasticizer content to adapt local material requirements with optimal fresh FSC mix characteristics. For FSC with recycled wastes, the cement was substituted in weight by 5%, 10%, and 15% SSP, and the natural sand was partially replaced in volume by GW at different percentages of 10, 20, 30, 40, and 50%. Details of the mix proportions of the FSC mixtures for 1 $m^3$ (by weight) and their mixture IDs are displayed in Table 3. As seen in Table 3 and described below, the mixture has the nomenclature SSPx + GWy, which includes x% cement substitution with SSP and y% fine aggregate (sand) substitution by GW. For example, $SSP_{10}$+$GW_{20}$ mixture refers to 10% cement replacement by SSP and 20% sand replacement by GW.

### 2.3. Mixing procedure and samples preparation

There is no specific mixing process for FSC. However, the adopted process was designed following self-compacting concrete guidelines [43]. Fig. 4 shows the mixing process of manufactured FSC mixtures. Three phases have been pursued in the mixing process of FSC mixtures: first, aggregates and powder (cement and SSP) were mixed for 30 s, and then 70% of the mixing water was added and mixed for 1 min. The remaining 30% of the superplasticizer-containing water was added and stirred for 1 min. The process went on for




**Fig. 1.** Fillers used in this study (a) cement, (b) marble powder, (c) seashell powder.

**Table 1**
Chemical composition and physical properties of cement, MP, and SSP.

| Chemical composition (%) | Cement | MP | SSP |
|---|---|---|---|
| $SiO_2$ | 23.83 | 0.27 | 0.11 |
| $Al_2O_3$ | 6.05 | 4.39 | 4.07 |
| $Fe_2O_3$ | 4.66 | 0.12 | 0. 1 |
| CaO | 56.35 | 94.31 | 95.06 |
| MgO | 2.44 | 0.56 | 0.22 |
| $K_2O$ | 0.83 | – | – |
| $Na_2O$ | 0.58 | – | – |
| $SO_3$ | 2.37 | 0.06 | 0.11 |
| LOI | 2.23 | – | – |
| Cl | – | 0.1 | 0.1 |
| *Physical properties* | | | |
| Specific density ($kg/m^3$) | 3110 | 2730 | 2880 |
| Blaine fineness ($m^2/kg$) | 3420 | 2700 | 8000 |

MP- Marble Powder, SSP- Seashell powder.

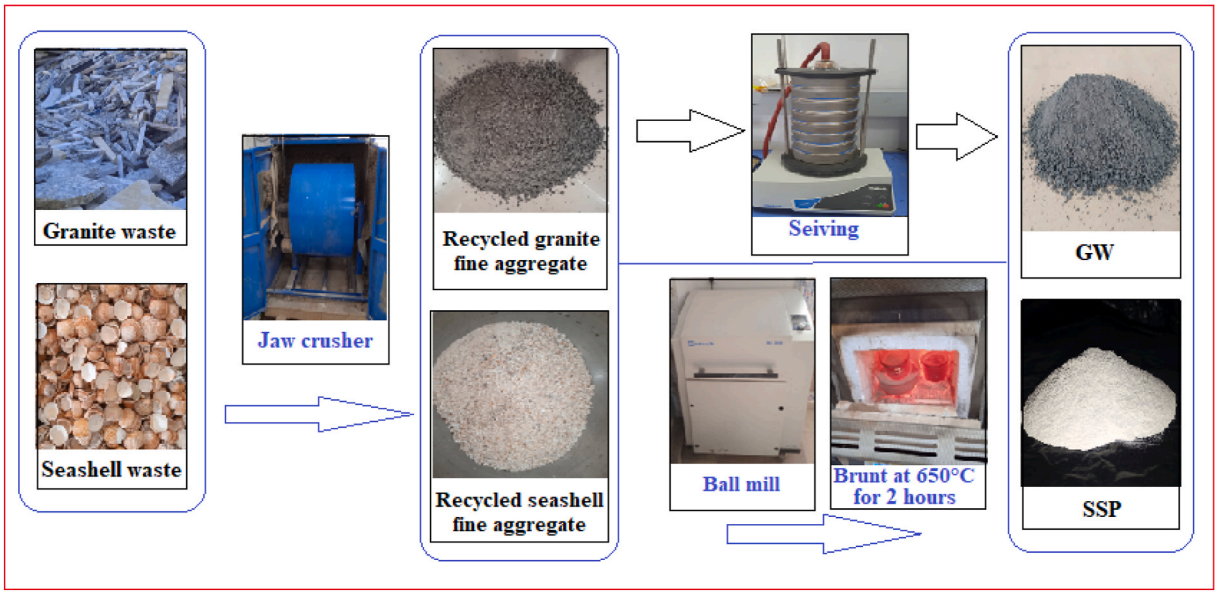



**Fig. 2.** Production process of recycled raw materials.




**Fig. 3.** Fine aggregates, (a) natural sand, (b) granite waste sand.

another 5 min before stopping for 3 min. At the end, the mixes were mixed for another minute to ensure FSC homogeneity [44].

After mixing, a total of 36 specimens were cast for each FSC mixture in lubricated steel molds without any vibration or compaction under laboratory conditions (at 20 °C and 50% relative humidity (RH)) to determine the physical, mechanical, and durability properties of hardened FSC mixes. For each FSC mix, 9 prismatic specimens with 40 × 40 × 160 mm were cast for compressive testing at 7, 28, and 90 days; 9 cylinder specimens with 160 mm diameter and 320 mm height were used to evaluate the modulus of elasticity at 7, 28, and 90 days; 9 cubic specimens with 100 mm dimensions were used to evaluate the ultrasonic pulse velocity at 7, 28, and 90 days;

**Table 2**
Chemical composition and physical properties of natural sand and GW sand.

| Chemical composition (%) | Natural sand | GW |
|---|---|---|
| $SiO_2$ | 90.35 | 51.29 |
| $Al_2O_3$ | 4.56 | 20.47 |
| $Fe_2O_3$ | 0.51 | 12.58 |
| CaO | 1.67 | 11.88 |
| MgO | 0.15 | 5.51 |
| $K_2O$ | 1.92 | 1.47 |
| $Na_2O$ | – | 1.36 |
| $SO_3$ | 0.7 | 0.27 |
| LOI | – | – |
| Cl | – | – |
| Physical properties | | |
| Specific density (kg/m$^3$) | 2630 | 2510 |
| Fineness modulus | 2.33 | 2.68 |
| Maximum size (mm) | 3.15 | 4.75 |
| Water absorption (%) | 0.96 | 4.34 |

**Table 3**
Mix proportioning of different FSC mixes.

| Mix. ID | Binder | | | Fine aggregate | | w/b ratio | SP (%) |
|---|---|---|---|---|---|---|---|
| | OPC (Kg/m$^3$) | MP (Kg/m$^3$) | SSP (Kg/m$^3$) | Sand (Kg/m$^3$) | GW (Kg/m$^3$) | | |
| Control | 400.86 | 201.93 | 0 | 1400 | 0 | 0.44 | 0.80 |
| $SSP_5$+$GW_0$ | 380.82 | 201.93 | 20.04 | 1400 | 0 | 0.44 | 0.75 |
| $SSP_5$+$GW_{10}$ | 380.82 | 201.93 | 20.04 | 1266.4 | 133.6 | 0.44 | 0.80 |
| $SSP_5$+$GW_{20}$ | 380.82 | 201.93 | 20.04 | 1132.8 | 267.2 | 0.44 | 0.80 |
| $SSP_5$+$GW_{30}$ | 380.82 | 201.93 | 20.04 | 999.2 | 400.8 | 0.44 | 0.80 |
| $SSP_5$+$GW_{40}$ | 380.82 | 201.93 | 20.04 | 865.6 | 534.4 | 0.44 | 0.80 |
| $SSP_5$+$GW_{50}$ | 380.82 | 201.93 | 20.04 | 732 | 668 | 0.44 | 0.80 |
| $SSP_{10}$+$GW_0$ | 360.78 | 201.93 | 40.08 | 1400 | 0 | 0.44 | 0.75 |
| $SSP_{10}$+$GW_{10}$ | 360.78 | 201.93 | 40.08 | 1266.4 | 133.6 | 0.44 | 0.80 |
| $SSP_{10}$+$GW_{20}$ | 360.78 | 201.93 | 40.08 | 1132.8 | 267.2 | 0.44 | 0.80 |
| $SSP_{10}$+$GW_{30}$ | 360.78 | 201.93 | 40.08 | 999.2 | 400.8 | 0.44 | 0.80 |
| $SSP_{10}$+$GW_{40}$ | 360.78 | 201.93 | 40.08 | 865.6 | 534.4 | 0.44 | 0.80 |
| $SSP_{10}$+$GW_{50}$ | 360.78 | 201.93 | 40.08 | 732 | 668 | 0.44 | 0.80 |
| $SSP_{15}$+$GW_0$ | 340.74 | 201.93 | 60.12 | 1400 | 0 | 0.44 | 0.75 |
| $SSP_{15}$+$GW_{10}$ | 340.74 | 201.93 | 60.12 | 1266.4 | 133.6 | 0.44 | 0.80 |
| $SSP_{15}$+$GW_{20}$ | 340.74 | 201.93 | 60.12 | 1132.8 | 267.2 | 0.44 | 0.80 |
| $SSP_{15}$+$GW_{30}$ | 340.74 | 201.93 | 60.12 | 999.2 | 400.8 | 0.44 | 0.80 |
| $SSP_{15}$+$GW_{40}$ | 340.74 | 201.93 | 60.12 | 865.6 | 534.4 | 0.44 | 0.80 |
| $SSP_{15}$+$GW_{50}$ | 340.74 | 201.93 | 60.12 | 732 | 668 | 0.44 | 0.80 |

MP- Marble Powder, SSP- Seashell Powder, GW- Granite Waste, SP (%) is calculated, in mass, compared to the binder mass.

and another 9 prismatic specimens with 40 × 40 × 160 mm were cast for porosity, water absorption, and acid attack.

After 24 h, all specimens were removed from the molds and immersed in water saturated with lime at 20 °C until specified testing ages. In order to attain a stable weight, all samples were taken out of the water tank 24 h prior to the testing day and dried in an electric oven set at 60 °C. For each experimental test and age, the average value of three identical specimens was taken as the result in the hardened state.

### 2.4. Testing

#### 2.4.1. Fresh tests

The fresh properties of FSC mixes, such as filling and passing capacity, as well as the ideal superplasticizer dosage giving satisfactory FSC blends without segregation or bleeding, were determined using the mini slump flow diameter and V-funnel flow time tests (Fig. 5) according to the EFNARC standard [43].

#### 2.4.2. Hardened tests

*2.4.2.1. Compressive strength, modulus of elasticity, and ultrasonic pulse velocity tests.* Compressive strength and modulus of elasticity were evaluated at 7, 28, and 90 days of curing on cubic specimens of 40x40 × 40 mm (Fig. 6-a) and cylindrical specimens of 160 × 320 mm (Fig. 6-b) according to standards EN 196-1 and ASTM C469-14 [45,46], respectively. In order to gain more information about the homogeneity and porosity of the FSC mixes, the ultrasonic pulse velocity (UPV) test was conducted as a non-destructive test at 7, 28, and 90 days of curing on cubic specimens of 100 mm, according to the ASTM C597-16 standard [47]. To measure the ultrasonic pulse velocity (UPV), the two ultrasound probes (transmitter and receiver) must be placed on the two ends of the specimens (Fig. 6-c). The following equation was used to calculate the UPV:

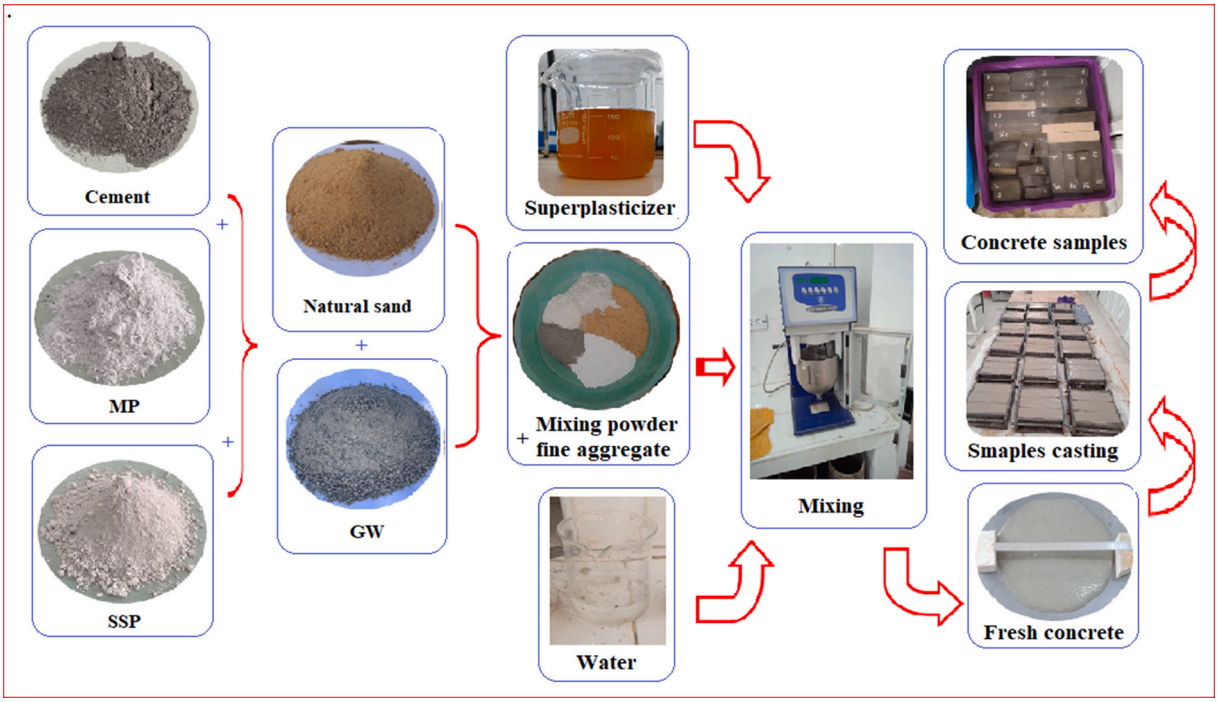



**Fig. 4.** Mixing process of FSC mixtures.



**Fig. 5.** Slump flow and V-funnel flow time tests.

$$UPV = \frac{L}{t} \tag{1}$$

Where L: Distance between the transmitter and receiver in (m); and *t*: time of wave propagation in (s).

*2.4.2.2. Porosity and water absorption tests.* Concrete porosity is considered one of the most important durability indicators. Three halves of prismatic specimens at least 90 days old (Fig. 7) were used to determine the void percentage in accordance with the ASTM C642 standard [48]. The capillary water absorption test was used to determine the sorptivity of the hardened concrete in accordance with the ASTM C642-13 standard [48]. For each mix, three prismatic specimens of 40x40 × 160 mm and more than 28 days of age were tested. The samples were oven dried for 24 h at 105 ± 5 °C before being submerged in a 5 mm sheet of water for 48 h. The procedure consisted of measuring the mass of each specimen repeatedly for 24 h until there was less than a 0.5% discrepancy in the measurements (Fig. 8).

*2.4.2.3. Acid attack test.* The acid-attack resistance of each mixture was studied to evaluate its durability. After 28 days of curing, the test specimens were weighed before being immersed in a 5 wt% hydrochloric acid solution (HCl) for 180 days at a temperature of 23 ± 2 °C. The samples were then weighed and crushed to determine the mass loss and compressive strength loss (Fig. 9) according to ASTM C307-03 standard [49]. The compressive strength loss and weight loss of the acid-attacked specimen were determined using the

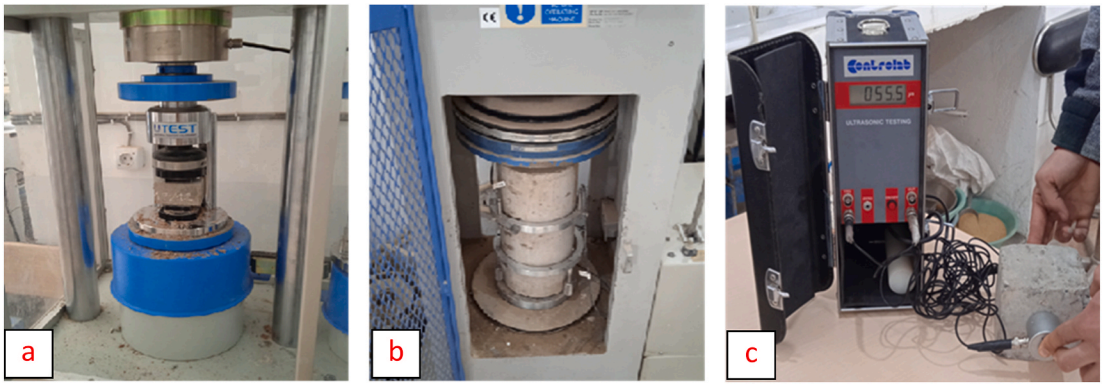



**Fig. 6.** Compressive strength, modulus of elasticity, and ultrasonic pulse velocity tests.



**Fig. 7.** Porosity test.

following formulas.

$$\text{Loss in strength } (\%) = \frac{fc\left(t_{day}water\right) - fc\left(t_{day}acid\right)}{fc\left(t_{day}water\right)} \times 100 \tag{2}$$

Where *fc ($t_{day}$ water):* Compressive strength of concrete specimens after t day's immersion in water; and *fc ($t_{day}$ acid)*: Compressive strength of concrete specimens after t day's immersion in acid;

$$\text{Loss in weight } (\%) = \frac{W\left(t_{day}water\right) - W\left(t_{day}acid\right)}{W\left(t_{day}water\right)} \times 100 \tag{3}$$

Where *W($t_{day}$ water):* initial weight of the of concrete specimens before t day's immersion in acid; and *W($t_{day}$ acid):* final weight of the




**Fig. 8.** Water absorption test.



**Fig. 9.** Immersion and appearance samples under acid attack.

concrete specimens after t day's immersion in acid.

*2.4.2.4. XRD, TGA and SEM analyses.* In order to evaluate the effects of SSP and GW incorporation on the microstructural properties and hydration development of FSC mixtures, the XRD, TGA, and SEM analyses (Fig. 10a-c) were performed on the hardened binder pastes of some FSC mixes with or without wastes.

Scanning electron microscopy (SEM) analysis was carried out using VEGA3-TESCAN SEM with a 25 KV accelerating voltage (Fig. 10-a) to study the morphology of raw materials and the microstructure of some hardened FSC mixtures, including hairline cracks, surface morphology, voids, and the interfacial transition zone (ITZ) between aggregate and cement paste. To make the sample electrically conductive, it was placed in a cuter, and a thin layer of gold was then applied.

X-ray diffraction (XRD) analysis was utilized for the determination of the mineral phase composition of both raw materials and FSC mixes. Samples for the XRD test were taken from the fragments for compressive strength testing at the age of 90 days. They were immersed in anhydrous ethanol to stop their hydration and then dried directly at 60 °C for 24 h. Subsequently, the cement paste was isolated from the surrounding sand and ground until the distribution of particle sizes was smaller than 80 μm. Following sample preparation, a mass of 2 or 3 g of prepared powder was obtained and subjected to the XRD test with an X-ray tube (Cu 1.54 Å) using a BRUKER, AXS, D8 instrument, as shown in Fig. 10 b. The diffractogram was obtained in a range of $2\theta$, between 20° and 90°, and at a rate of 1 s for 50 min.

Thermogravimetric analysis (TGA) was performed to examine the hydration products by observing changes in the hardened FSC utilizing the SHIMADZU DTG-60/60H instrument (Fig. 10c) for samples weighing approximately 10 mg. The tested samples come from the same samples prepared for the XRD test. The degree of hydration is estimated by determining the mass loss due to the decomposition of calcium carbonate ($CaCO_3$), calcium hydroxide ($Ca(OH)_2$), and calcium silicate hydrate (C–S–H) at temperatures between 100 and 900 °C from the TGA and DTA curves, respectively.

## 2.5. Environmental impact assessment

As is known, cement production and conventional aggregate extraction produce a large amount of $CO_2$ as compared to other concrete components, which adds a significant amount to the global emissions from energy and industrial sources. During its cycle, concrete production goes through three main phases, as shown in Fig. 11. The $CO_2$ footprint calculation in this research is limited to cement production (production of clinkers) and conventional aggregate extraction phases. The $CO_2$ produced was calculated from one cubic meter of concrete manufacturing. The volume of raw material consumption (cement and natural river sand) derived from the proportions of various FSC mixtures (Table 3), and the $CO_2$ emission factor are used to assess the environmental impact. In this study, the $CO_2$ emission factors obtained from the results of Sudjono and Yudhi [50] are 1.77 kg $CO_2$/kg for ordinary Portland cement and 0.37 kg $CO_2$/kg for natural river sand. For all FSC mixtures, the calculated values of emitted $CO_2$ were cumulative from cement and natural sand [51].




**Fig. 10.** Microstructural tests, a- SEM analysis, b- XRD analysis, c- TGA analyses.

## 3. Results and discussion

### 3.1. Characterization of raw materials

#### 3.1.1. Cement, marble powder and seashell powder

According to Table 1, the chemical compositions of cement, MP, and SSP are 23.83, 6.05, 4.66, and 56.35 wt%; 0.27, 4.39, 0.12, and 94.31 wt%; and 0.11, 4.07, 0.1, and 95.06 wt%, respectively, for $SiO_2$, $Al_2O_3$, $Fe_2O_3$, and CaO as major oxides contained in cement and mineral stone waste. Referring to the percentage of $SiO_2$ in the MP and SSP (0.27 and 0.11 wt%), and the XRD analysis of SSP presented in Fig. 12 a, it was revealed that the mineralogical compositions of the MP and SSP include calcium oxide (CaO) and calcium hydroxide ($Ca(OH)_2$), which demonstrated their essentially limestone nature (see Fig. 13).

According to the results shown in Table 1, the MP was found to have the lowest specific density with a value of 2.73 g/cm$^3$, followed by the SSP (2.88 g/cm$^3$) and cement (3.11 g/cm$^3$). The specific surface area values are 3420 cm$^2$/g, 2700 cm$^2$/g and 8000 cm$^2$/g, respectively, for cement, MP, and the SSP. The morphology of SSP particles, as inferred from Fig. 2a, is angular with an irregular and rough surface texture, which allows the cement paste to adhere better to the aggregates.

#### 3.1.2. Natural sand and GW sand

As presented in Table 2, the main chemical compositions forming the natural sand are 90.35% $SiO_2$, 1.67% CaO, 4.56 $Al_2O_3$, and 0.51% $Fe_2O_3$, while the main oxides forming the GW are 51.29% $SiO_2$, 11.88% CaO, 20.47% $Al_2O_3$, and 12.59% $Fe_2O_3$. By referring to the $SiO_2$% of natural sand and GW (90.35 and 51.29 wt%) and their XRD analysis presented in Fig. 12b and 12 c, it was revealed that the major crystalline phases of the natural sand and GW were quartz, albite, and microcline, which demonstrated their essentially siliceous nature.

From Table 2, the specific densities (SD) of natural sand and GW were 2.63 g/cm$^3$ and 2.51 g/cm$^3$, respectively. The water absorption value for GW was 4.34%, which is more than four times that of 0.96% for natural sand. These values indicate the high porosity of GW compared to natural sand. The SEM investigation shown in Fig. 12 c reveals the rounded shape and smooth surface of natural sand grains. However, the GW sand grains exhibit an angular shape and a rough surface (Fig. 3a–b), which provide a good bond between the cement paste and aggregates compared to natural sand.

Regarding the particle size distribution of natural sand and GW sand shown in Fig. 14, results indicate a continuous particle size distribution ranging from 0.08 to 3.15 mm and 0.08–4.75 mm for natural sand and GW, respectively. However, the curve for natural sand was seen to be slightly finer than that of crushed GW. Both materials were seen to meet the nominal aggregate size range for use as fine aggregate in concrete, according to EN 1097-6 [52]. The fineness modulus of natural sand and GW sand were 2.33 and 2.68, respectively.

### 3.2. Characterization of fresh FSC mixtures

The slump flow results of fresh FSC mixtures are presented in Fig. 15. This figure indicates that the slump flow of all FSC mixtures is between 270 and 320 mm, which shows good deformability in accordance with the EFNARC recommendations [43]. A significant increase in the slump flow diameter was observed with the increasing content of SSP and decreasing rate of GW, especially for mixtures containing 50% GW, compared to control FSC. This improvement in the flow of SSP-based mixtures may be due to the delayed reaction of seashell powder with water compared to cement. In addition, the high CaO content of SSP (Table 1) may result in a longer than expected initial setting time caused by the dilution effect of the seashell, resulting in additional free water [10,25,53]. The decrease in slump flow of mixes with GW was due to the rough and angular morphology of GW (Fig. 12d), as well as its higher water absorption compared to natural sand (Table 2). These findings were in line with the outcomes of previous research on the use of granite waste aggregates [38,54,55]. Karimipour et al. [56] declared the same reason for reducing the workability of SCC when GW was used as filler to replace cement content. According to Lin et al. [57], aggregates with a large surface area and high water absorption absorb part of the mixing water, consequently decreasing the flowability of mortar. As a result, all FSC mixtures demonstrated acceptable slump flow diameter with a constant superplasticizer dosage by adding a combination of GW and SSP.

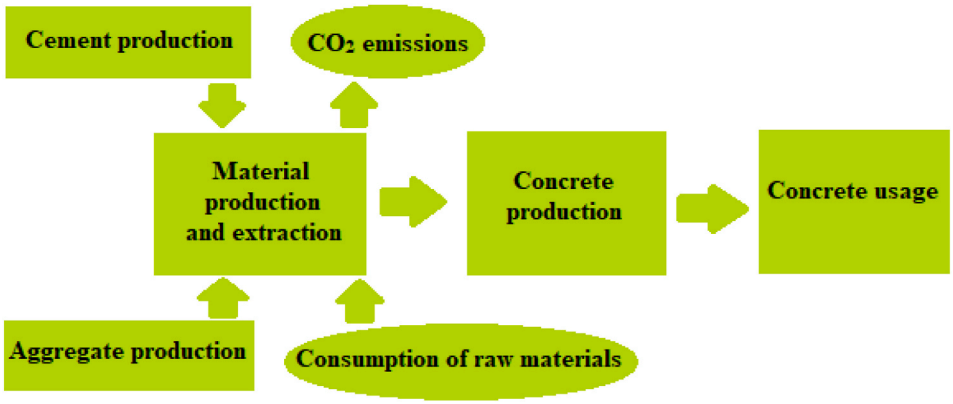



**Fig. 11.** Schematic of cycle concrete production including environmental impact assessment.

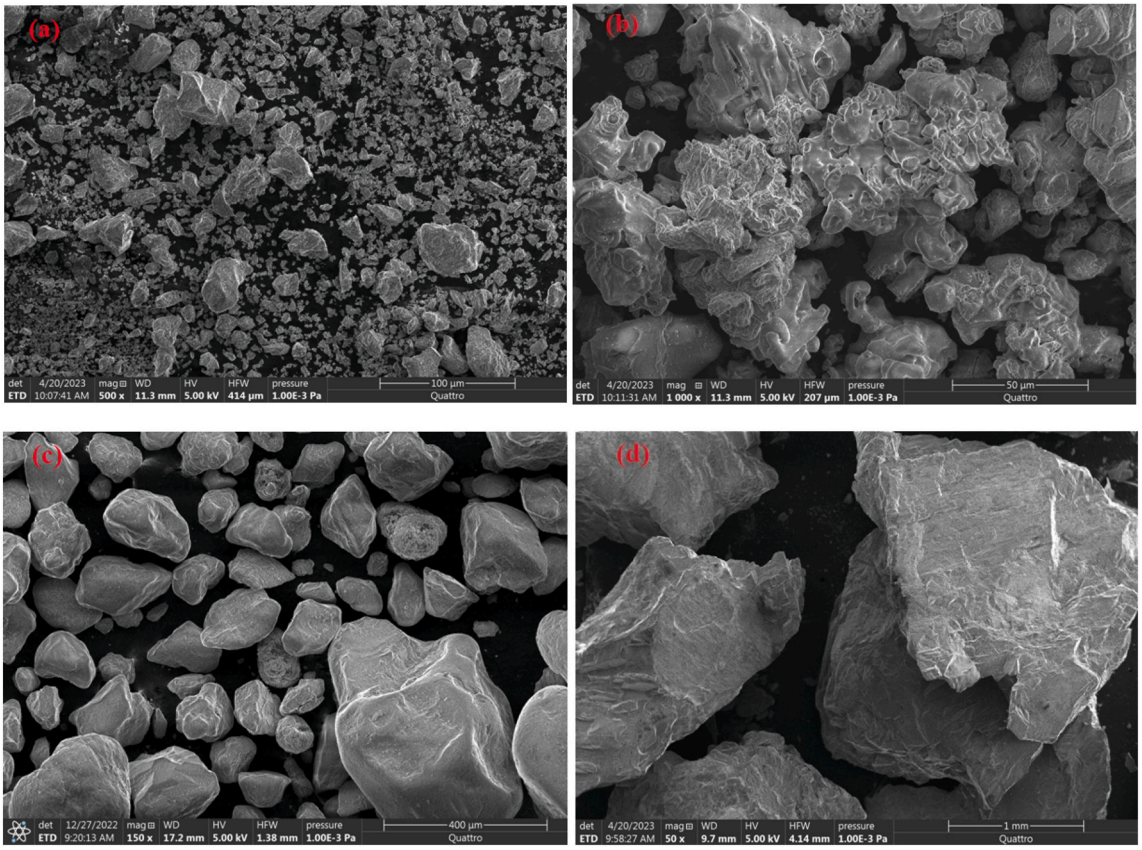



**Fig. 12.** SEM image of cement (a), seashell powder (b), natural sand (c) and GW (d).

Similarly to the slump flow diameter, the results of the V-funnel flow time test displayed in Fig. 16 demonstrate that the flow times of all FSC mixtures were acceptable and less than the EFNARC recommended value of 10s [43]. The addition of SSP decreased the flow time and viscosity of FSC mixes. In addition, because the hydration of SSP takes longer than the hydration of OPC, the mixtures needed the same quantities of water and superplasticizers as the control mixture to have the desired flowable properties [58,59]. Moreover, the flow time increased when GW was used as natural sand. Among all the mixtures incorporating SSP combined with GW, the optimum flow times happened when 15% of SSP and 10% of GW were added to the mixture with a lower flow time value and a similar amount of SP to that for the control mixture (0SSP+0 GW). On the other hand, the longest flow times are registered after the simultaneous addition of 5% SSP and 50% GW.

### *3.3. Characterization of FSC mixtures in hardened state*

#### *3.3.1. Compressive strength*

Fig. 17 shows the variation in compressive strength results for the different FSC mixtures at 7, 28, and 90 days. It can be seen from this figure that the compressive strength increases as the percentage of SSP rises. However, there was a reduction in strength over 15% SSP content compared to 5% and 10% SSP contents. For instance, the 7-day compressive strength of the 0SSP+0 GW FSC mixture was 25.21 MPa and became 26.82 MPa, 27.19 MPa, and 25.96 MPa for FSC mixtures prepared without GW and with 5%, 10%, and 15% SSP, respectively. This might be because the hydration process is developed, and as a result, the strength of FSC starts to increase with curing. Similarly, the compressive strength of FSC mixes at 90 days also rises from 39.97 MPa to 41.17 MPa, 44.93 MPa, and 40.57 MPa, showing increases in strength of 2.91%, 11.03%, and 1.47%, respectively, above the control FSC. This increase in strength with the addition of SSP at 90 days is explained by the formation of calcite that took place after the hydration process and consists of the observations found by Gong et al. [60]. The resulting strength was contributed with the help of pozzolanic reactions and carbonate compound production [10,61]. Regardless of the curing times, the results showed that the optimum amount of compressive strength was developed for the mixtures with 10% SSP. This decrease in compressive strength of the mixture with 15% SSP compared to those with 10% may be caused by the high concentration of CaO in SSP, which might react with gypsum and $Al_2O_3$, reducing the early hydration of the alite [17,62]. Okoro and Oyebisi [9] also found that 10% cement replacement with seashell provided the best geopolymer compressive strength for 3, 7, 14, 28, and 56 curing days; and more than 10% of replacement resulted in a strength decline. It should be noted that despite the reduction in strength for FSC mixtures with 15% SSP compared to those with 5 and 10% SSP, it remained greater than that of the control mixture.

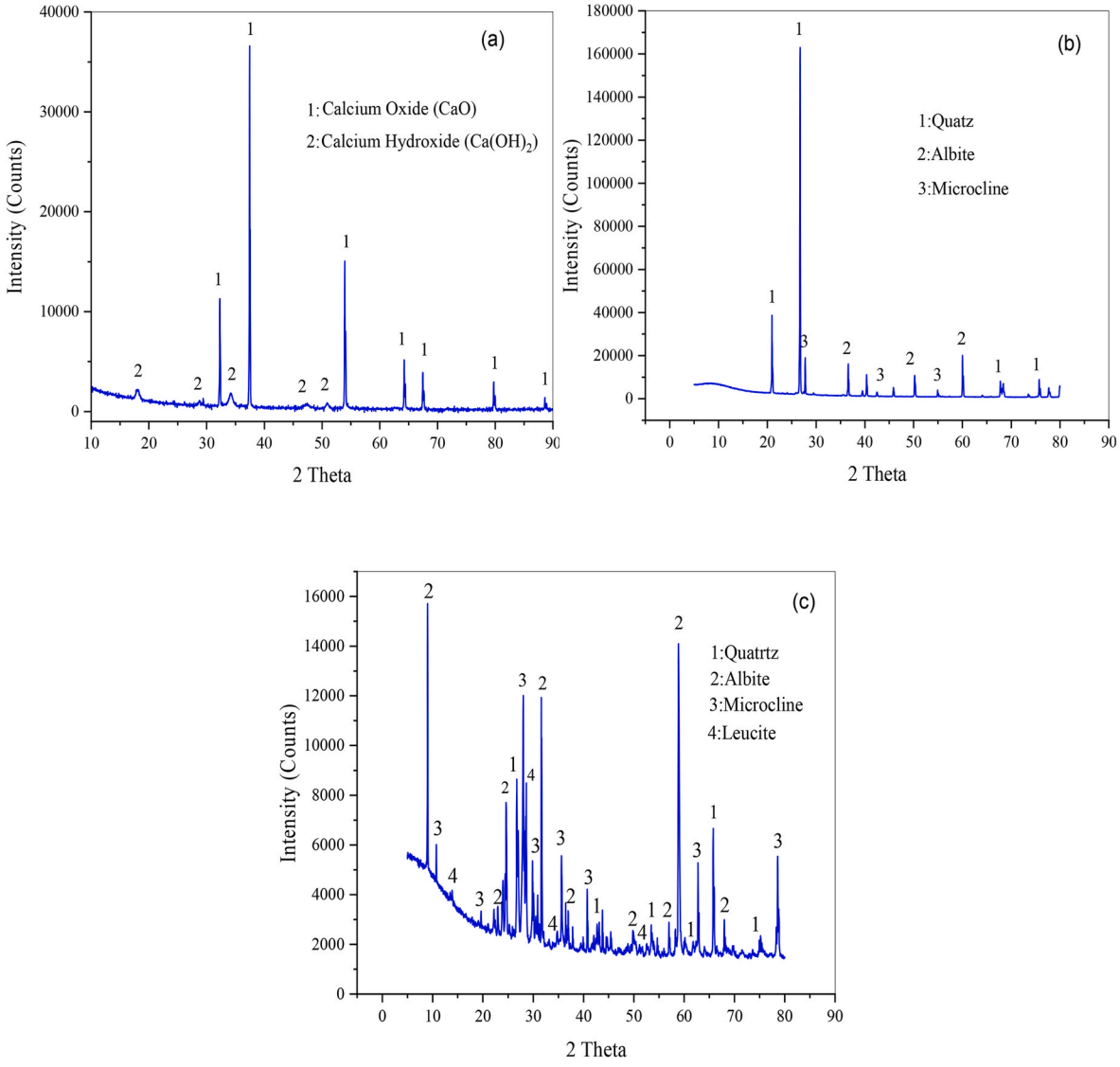



**Fig. 13.** X-ray diffraction analysis of SSP (a), natural sand (b) and GW (c).

Furthermore, Fig. 17 shows that the addition of GW increases the compressive strength of FSC mixes. For instance, at the age of 90 days, the strength increases from 39.97 MPa for control FSC to 63.22 MPa, 66.51 MPa, and 61.91 MPa for mixtures 5SSP+50GW, 10SSP+50GW, and 15SSP+50GW, respectively, with an improvement of about 58.17%, 66.40%, and 54.89%. This increase in strength may be attributable to the angular shape and rough surface of GW particles (Fig. 1d), which enhance the interfacial transition zone between the cement paste and the aggregates, and, on the other side, to the filling of the pores by the SSP [63–66]. The increase in compressive strength using GW as fine aggregates was similar to findings reported by other researchers [55–57,67]. Binici and Aksogan [37] found an increase of about 3%, 4%, and 7% in the compressive strengths of the samples incorporating 10% granite aggregates at the end of 7, 28, and 90 days, respectively. Nuaklong et al. [38] also found an increase of about 27% and 40% in the 7-day and 28-day compressive strengths of geopolymer concrete with 50% granite waste as fine aggregates. They attributed this enhancement to the improved physical bond between the angular-shaped granite particles and the paste. Ahmadi et al. [66] found an increase of 8% in the compressive strength of foamed concrete containing sand from granite waste.

### *3.3.2. Ultrasonic pulse velocity (UPV)*

The UPV test is used to evaluate concrete quality and helps assess its durability. It is strongly linked to internal porosity, cracks, and microstructure variation [68]. Fig. 18 displays the effect of SSP and GW on the UPV of FSC mixtures at 7, 28, and 90 days of age. According to Malhotra et al. [69], concrete that has a UPV value greater than 3500 m/s is said to have good durability. As shown in Fig. 8, at all ages, the UPV results for all FSC mixes exceeded 3500 m/s, indicating that concrete produced using SPP with GW fine aggregates has good durability.

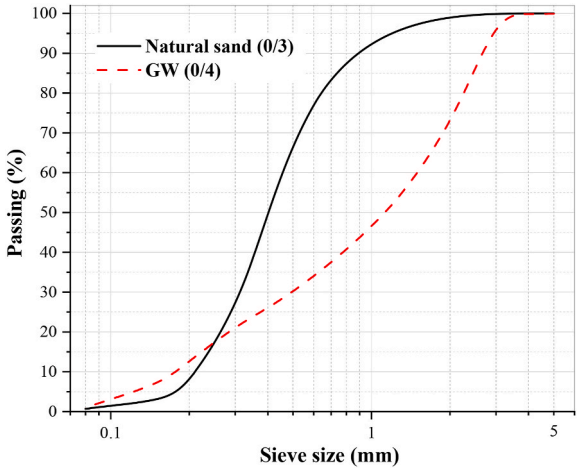



**Fig. 14.** Particle size distribution of fine aggregates.

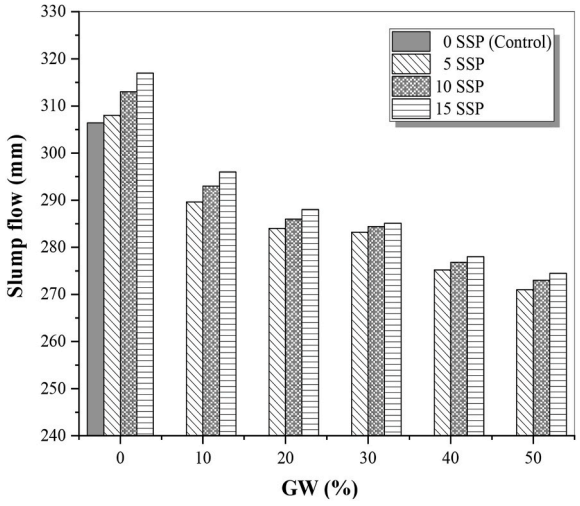



**Fig. 15.** Slump flow of FSC mixtures.

The results of this figure show that, as the percentage of GW increases, the UPV values increase. For instance, the values of 28-day UPV for 5SSP+50GW, 10SSP+50GW, and 15SSP+50GW mixtures are 4110.02 m/s, 4171.56 m/s, and 3964.7 m/s, respectively, with an increase of about 7.94%, 9.30%, and 4.57% with respect to control FSC (3785 m/s). This improvement in UPV values by the addition of GW is very advantageous for structural concrete and may be related to the reduction in the porosity of the mixtures as well as to the hardness of GW compared to natural sand. A similar enhancement in UPV was seen by Binici and Aksogan [37] when granite waste is used instead of sand.

It can be seen from the results of Fig. 18 that for all mixes and ages, the mixtures with 10% SSP show the greatest improvement in UPV compared to mixes with 5 and 15% SSP. Fig. 19 shows the linear relationship between the 90-day UPV values and compressive strengths of all FSC mixtures. This figure demonstrates that there is a good linear relationship between the improvement in the compressive strength and the increase in UPV with a strong coefficient of correlation (i.e., $R^2 = 0.859$) for FSC mixtures based on SSP and GW.

### *3.3.3. Modulus of elasticity*

The modulus of elasticity (E) is an important concrete characteristic to determine the extent of structural deformation for service requirements. The initial and later age modulus of elasticity are useful to know the elastic shortening and camber of the element at the time of the release of the prestress and to predict the creep coefficient for calculating losses in prestressed concrete members and the deflection of the reinforced concrete members, respectively.

The results of the modulus of elasticity test at 7, 28, and 90 days for mixtures made with SSP and GW are shown in Fig. 20. This figure illustrates the positive effect of using SSP with GW on the modulus of elasticity of FSC mixtures. For instance, the modulus of elasticity passed from 33.15 GPa for the control FSC to 38.20 GPa, 40.16 GPa, and 37.00 GPa for FSC mixtures prepared with

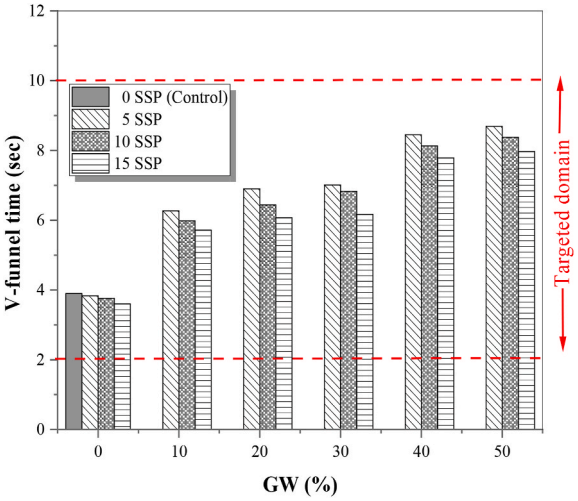



**Fig. 16.** V-funnel flow time of FSC mixtures.

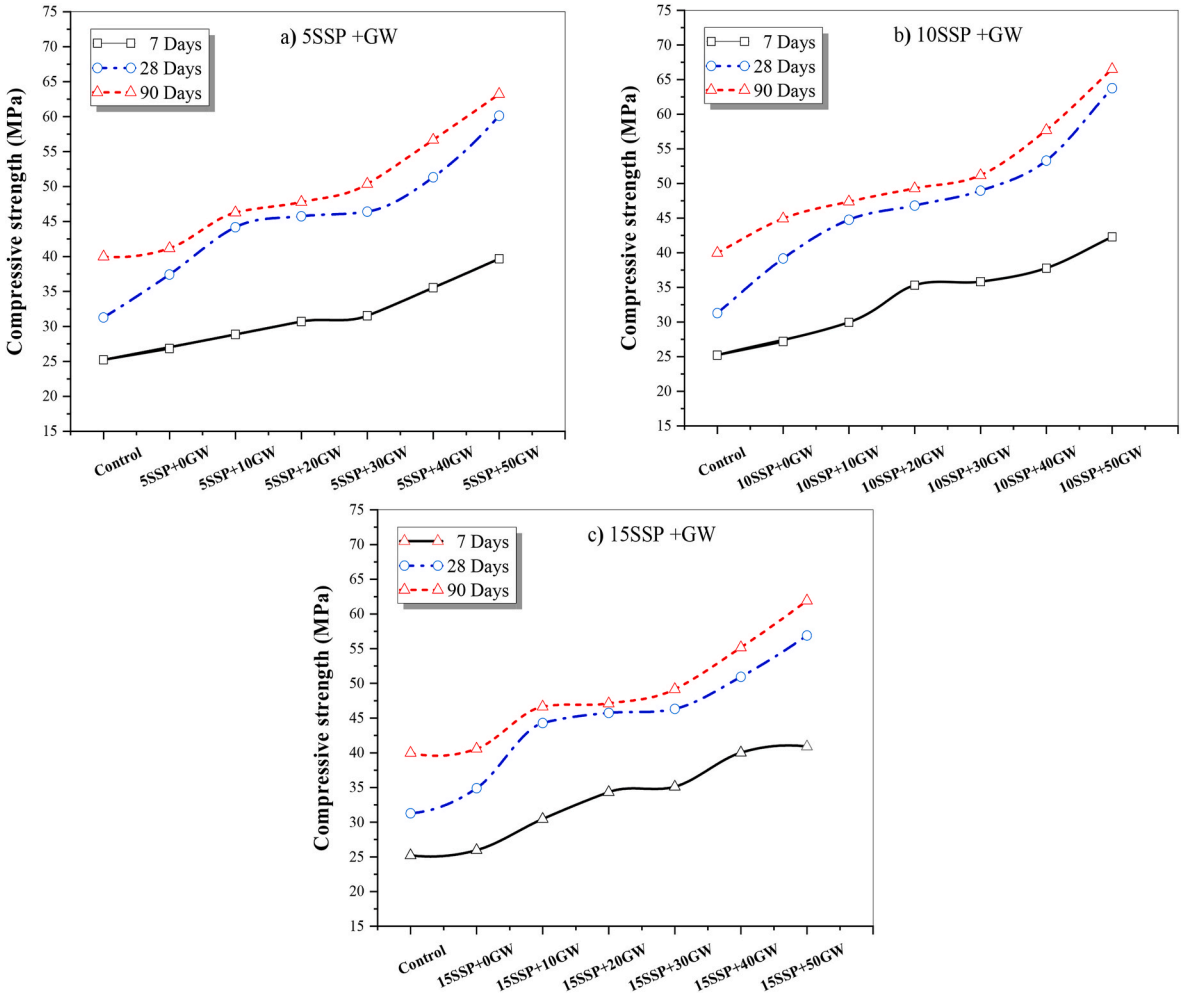



**Fig. 17.** Compressive strength of FSC mixtures.

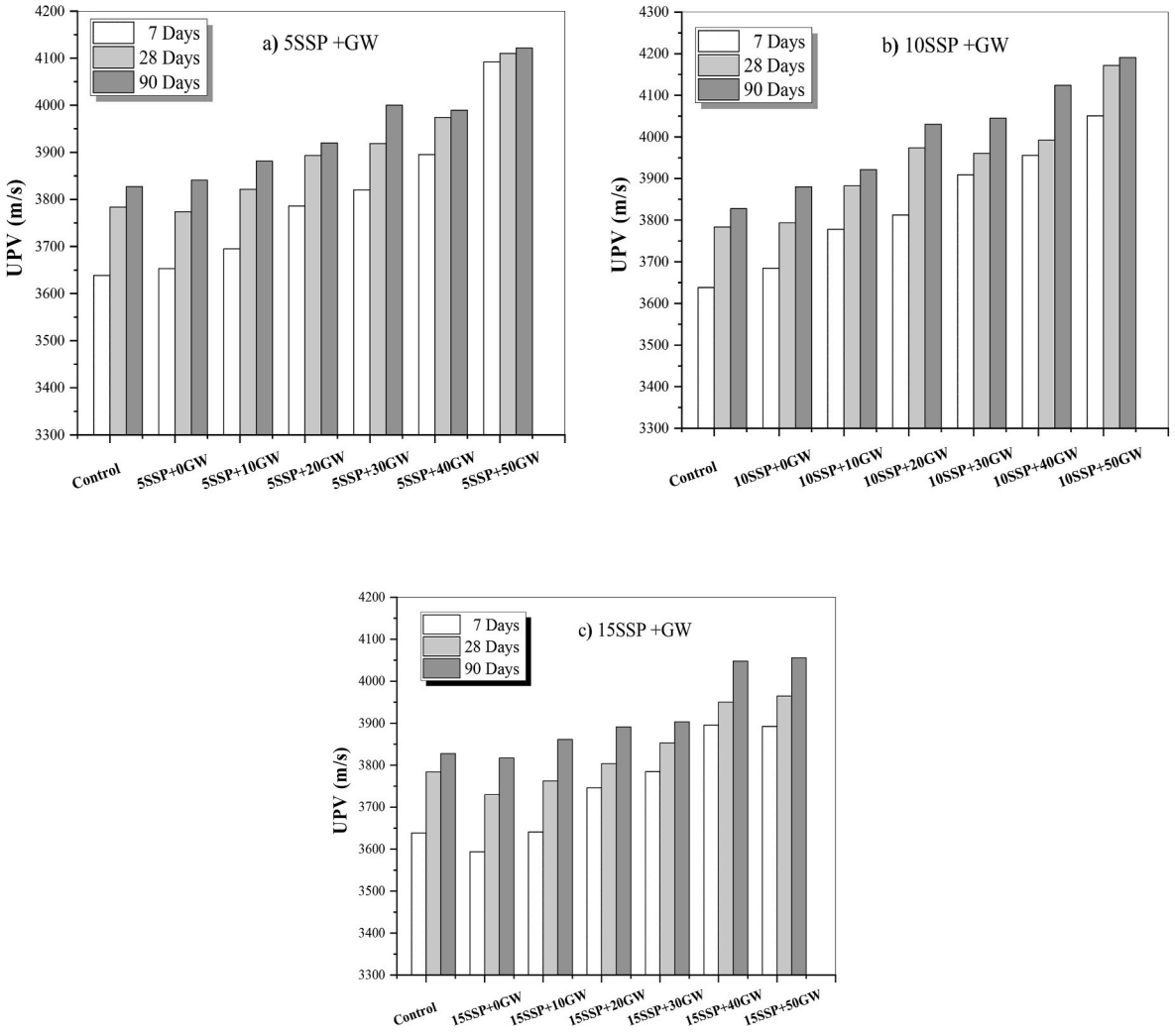



**Fig. 18.** Ultrasonic pulse velocity of FSC mixtures.

5SSP+50GW, 10SSP+50GW, and 15SSP+50GW, respectively. This trend is comparable to the rise in compressive strength that occurs as the amount of SSP and GW increases. The enhancement in the modulus of elasticity is attributed to the increased compressive strength caused by the fineness of the SSP, which can fill more pores and compact the microstructure (strong ITZ between the GW and the cement paste) [70]. On the contrary, Olivia et al. [71] and Tayeh et al. [72] found a reduction in the modulus of elasticity of concrete by adding SSP as a cement replacement. It is also observed from Fig. 20 that, for all ages, the modulus of elasticity increases proportionally with the increase in the GW in FSC mixtures. Where, when SSP is present at 5, 10, and 15%, the modulus of elasticity of FSC mixes with 50% GW is found to have the highest values and increases by about 13.21%, 17.45%, and 10.40%, compared to the control FSC. According to Pellegrino and Gaddo [73], greater cohesion between the cement matrix and aggregates resulting from the great roughness of crushed aggregates may produce greater rigidity in the concrete.

In addition, for all percentages of GW, mixtures with 10% SSP show better improvement in modulus of elasticity for all ages than mixtures with 5% and 15% SSP. Fig. 21 displays the relationship between the modulus of elasticity and the compressive strength of all the FSC mixtures at 90 days. It can be seen from this figure that there is a strong correlation between the compressive strength and the elastic modulus of FSC, which contains SSP and GW ($R^2 = 0.8$). According to Wu et al. [70], the larger crushing index of GW than that of NS increases the elastic modulus.

### *3.3.4. Porosity*

Fig. 22 shows the impact of SSP and GW on the porosity variation of all FSC mixtures at 90 days. The results display a decrease in porosity as the percentage of GW increases. For the control FSC mixture, the porosity was 5.37% and decreased to 4%, 2.95%, and 4.18% for FSC mixtures prepared with 5SSP+50GW, 10SSP+50GW, and 15SSP+50GW, respectively. This shows that the SSP positively reduces porosity. This decrease in porosity is due to the increase in hydration products formed by the pozzolanic reaction resulting from the high CaO content of the SSP, which fills the pores more [74]. Liu et al. [75] also reported that the replacement of

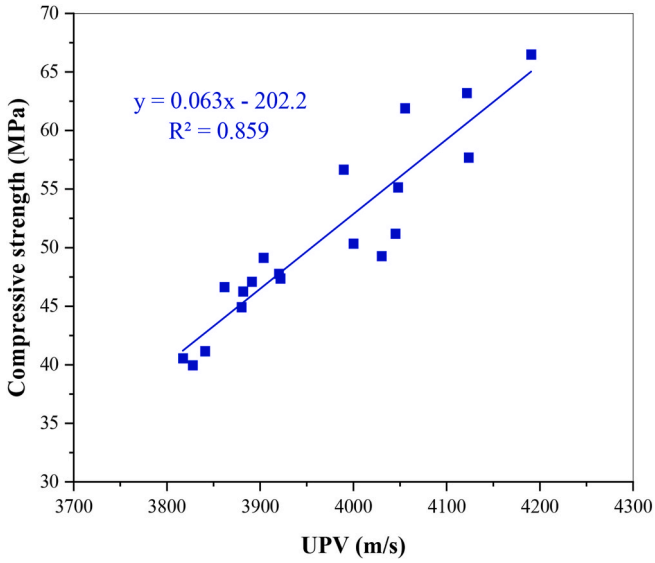



**Fig. 19.** Correlation between compressive strength and UPV of FSC mixtures.

cement with seashell powder decreased porosity. However, the addition of 15% SSP led to an increase in porosity compared to mixtures with 5% and 10% SSP. This may be due to the long hydration when an important quantity of cement was replaced. In Fig. 23, the results of the 90-day compressive strength and UPV test are plotted as a function of their corresponding porosities. This figure shows good linear relationships between strength, UPV, and the porosity of FSC containing SSP and GW, with high correlation coefficients between them ($R^2 > 0.8$).

### *3.3.5. Water absorption*

Water absorption by capillarity can be used as an indicator for determining the microstructure of concrete or mortar. The denser the mortar or concrete, the less capillary water absorption. The results of the 28-day water absorption of FSC mixtures containing different percentages of SSP and GW are displayed in Fig. 24. All concrete mixes satisfy the requirements of water absorption, with a maximum limit of 6% when compared to the specifications of concrete paving units [76]. The absorption of the control FSC mixture without GW and SSP (0SSP + 0GW) is 3.63% and decreases to 3.54, 3.4, and 3.61% for FSC mixtures without GW when the replacement of SSP is 5, 10, and 15%, respectively. This decrease in water absorption of FSC mixtures containing SSP is due to the reduction in porosity resulting from the filling effect of the SSP in the pores [77,78]. However, it seems from Fig. 24 that adding SSP at a lower substitution rate (5 and 10 wt%) results in less water absorption than for 15 wt% because the SSP particles fill the voids in the concrete matrix by interlocking with one another. Nevertheless, at higher replacement levels, the aragonite and rough morphology of SSP particles cause higher voids, leading to increased water absorption. Similar results were also found by Liao et al. [79], who found water absorption decreased as the content of SSP increased.

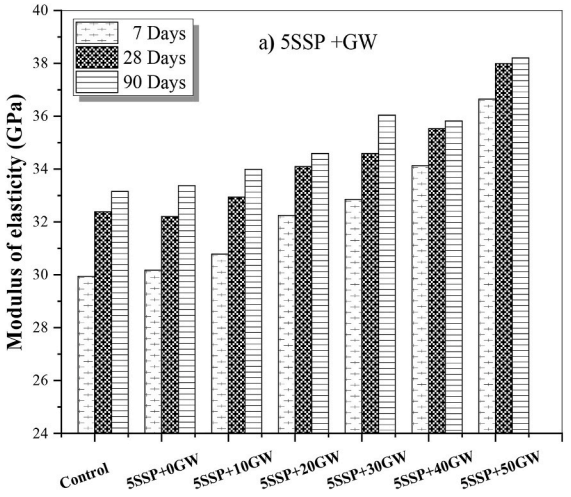
Moreover, it is clearly shown from Fig. 24 that the water absorption decreases proportionally with the increasing rate of GW, and the mixture with 50% replacement has the lowest water absorption. This decrease in water absorption by adding GW may be due to the low porosity and denser microstructure of FSC mixtures, resulting from the rough morphology and angular shape of GW [80]. A similar drop in capillary water absorption was found by Lin et al. [57] with the replacement of natural sand with GW sand. According to Binici and Aksogan [37], concrete with 10% granite aggregates had a capillary absorption coefficient that was 32% lower than the control concrete. In contrast, Vijayalakshmi et al. [34] found an increase in water absorption in concrete by adding granite powder.

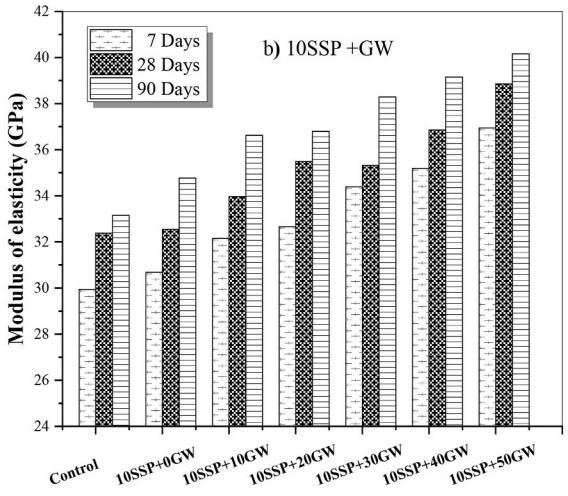
According to Das and Rout [81], the water absorption of a mixture is related to the surface porosity as well as the structural pores of cement paste. It can be confirmed by the SEM microstructure analysis, described in Fig. 25, that the water absorption in FSC specimens is correlated with the presence of pores. Fig. 14 illustrates the relationship between water absorption and porosity for all FSC mixtures. According to this figure, it can be seen that the increase in water absorption is associated with an increase in the porosity of the mixture, with a strong coefficient of correlation ($R^2 = 0.8$).

### *3.3.6. Acid attack*

Acid attack resistance is a property that is a good indicator of the durability of concrete in an aggressive environment. The results of the losses in mass and strength of FSC mixtures exposed to acid attacks are shown in Fig. 26(a–c). It is observed that the mass loss and strength loss values of the FSC mixtures with SSP and GW are substantially lower than those of the control FSC and decrease proportionally with the increase in the percentages of SSP and GW. Ghorbani et al. [82] found similar results, indicating that adding granite waste to concrete improved its resistance against acid and chloride attacks.

According to the obtained result, the mass loss and strength loss of the 5SSP+50GW, 10SSP+50GW and 15SSP+50GW mixtures are 3.98%, 3.29%, and 4.34% of mass loss, and 21.01%, 14.27%, and 17.23% of strength loss, respectively, which are weak as compared to



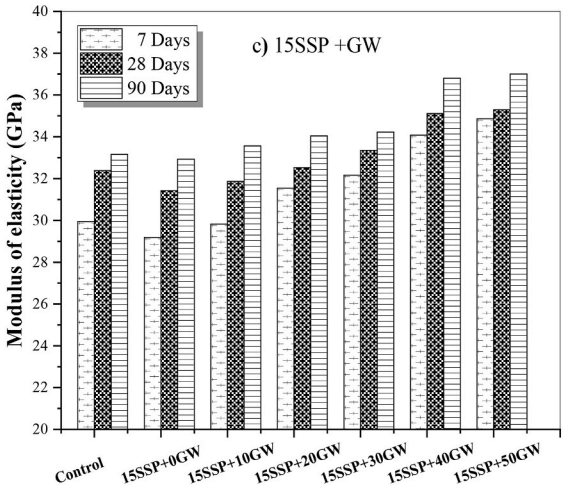




**Fig. 20.** Modulus of elasticity of FSC mixtures.

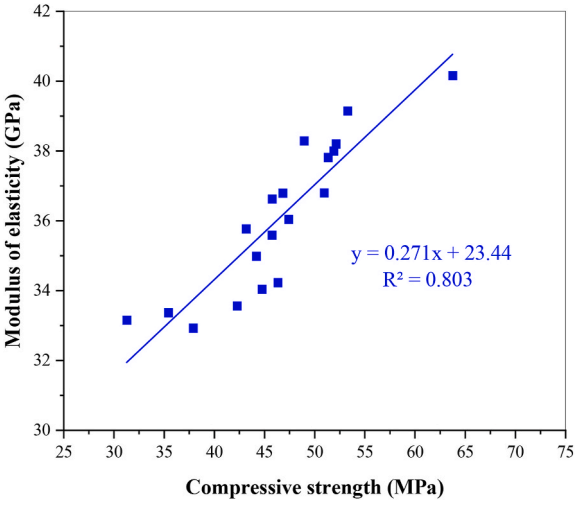



**Fig. 21.** Correlation between modulus of elasticity and compressive strength of FSC mixtures.

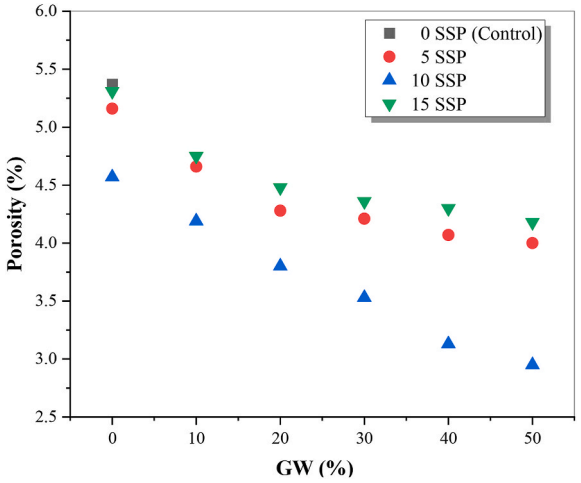



**Fig. 22.** Porosity results of FSC mixtures.

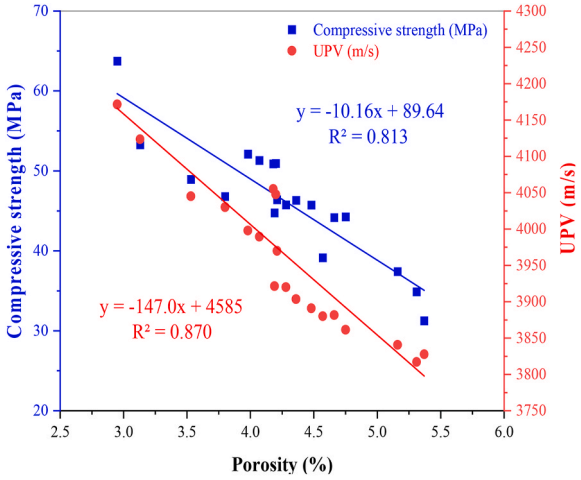



**Fig. 23.** Correlation between porosity, compressive strength and UPV of FSC mixtures.

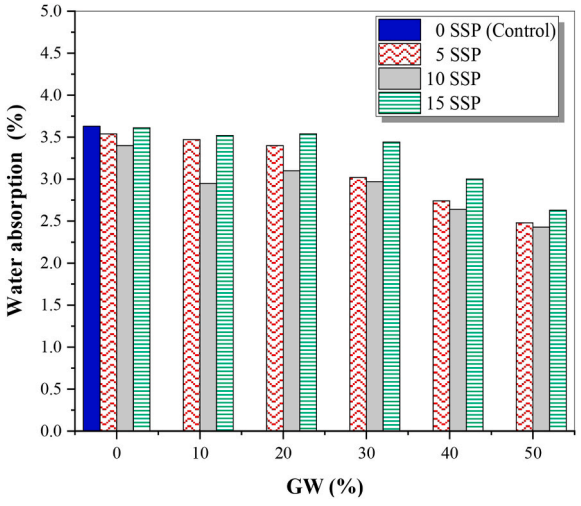



**Fig. 24.** Water absorption of FSC mixtures.

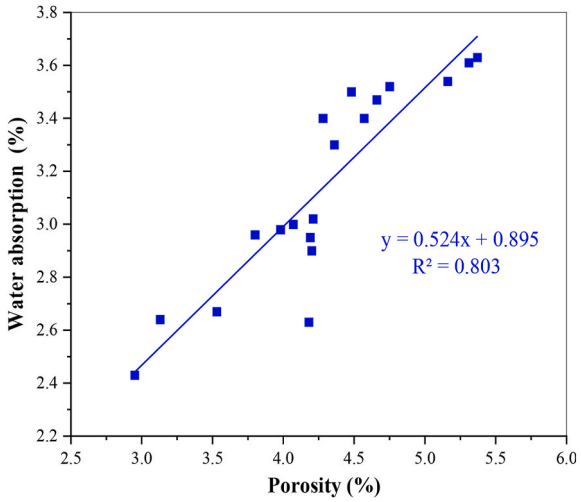



**Fig. 25.** Correlation between porosity and water absorption of FSC mixtures.

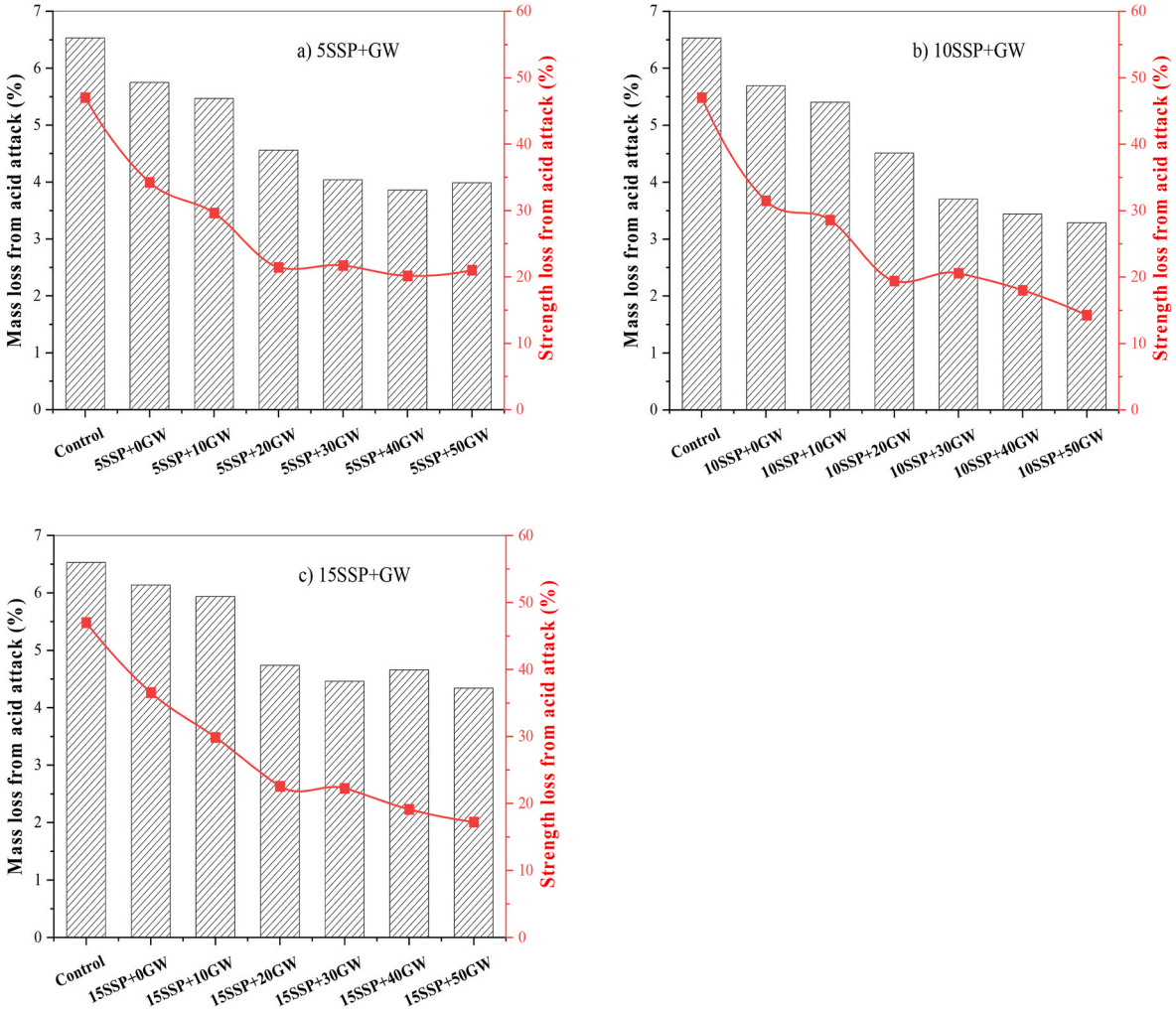



**Fig. 26.** Mass loss and strength loss of FSC mixtures after acid attack.

6.50% and 47% of the control FSC mixture. It can be concluded that mixtures with 10% SSP have the best acid resistance (lower mass loss and strength loss) than other mixtures, indicating that the addition of SSP is more efficient in improving the resistance to acid attacks in FSC mixtures. This can be explained by the weak absorption of FSC mixtures due to the reduction in pores size assumed by the filling effect of the SSP with high fineness (8000 $cm^2/g$). Qasem et al. [83] also reported that the use of 10% cockle shell powder in concrete has the best resistance to acid attacks compared to the mixture containing only cement. The relationship between mass loss and strength loss of FSC against acid attack is shown in Fig. 27. It is clearly observed from this figure that the increase in mass loss is associated with the increase in strength loss, with a high coefficient of correlation ($R^2 = 0.83$).

### 3.3.7. XRD analysis

The impact of seashell powder incorporation on the hydration process of FSC mixtures was examined through the XRD analysis of hardened samples after 90 days of curing. The XRD patterns of the control FSC and mixes made with 50% GW combined with 5%, 10%, and 15% SSP, respectively, are displayed in Fig. 28. The analysis was conducted using a scan range of 20–90° along two theta angles. The main peaks presented in the four FSC mixtures are calcite ($CaCO_3$), calcium hydroxide ($CaOH_2$), and calcium oxide (CaO), whose origin is linked to the composition of the SSP and hydration products of the cement used. However, the XRD spectra of the C–S–H gels show a weak peak intensity that is difficult to characterize. There is a slight difference between the XRD patterns of the control FSC and the mixtures containing SSP, except the portlandite ($Ca(OH)_2$), calcium oxide (CaO), and calcite ($CaCO_3$) peaks. Calcium is found in pure and hydrated as calcium oxide and calcium hydroxides in FSC mixtures, which contribute to the formation of a hardened network and give rise to high strength [84]. According to Okoro et al. [9], calcium hydroxide, which is formed by the combination of calcium oxide (CaO) and water ($H_2O$) during hydration, increases mechanical strength. It is shown in Fig. 28A that the peak intensity of Ca $(OH)_2$ first increased and then decreased with increasing SSP replacement cement ratio from 0 to 15%. The levels of $Ca(OH)_2$ in FSC with 10% SSP and 50% GW were more intense than those in mixture with 15% SSP and 50% GW. Additionally, portlandite was formed as a primary product of the hydration process along with C–S–H gels [10]. Up to 10% of cement substitution, the addition of SSP to FSC increases the formation of portlandite ($Ca(OH)_2$) and calcium oxide (CaO), and therefore, the crystallinity of the mixture increases, due to the reaction of calcium oxide (CaO) with water and $SiO_2$ to generate C–S–H and CH. Research indicates that adding seashell powder to blended cement results in a new hydrated cement matrix with enhancing cohesiveness and integrity. The SSP increases the precipitation of hydration products, especially prtlandite and C–S–H, by enhancing the hydrated cement matrix, which could be explained by a strength increase result [25,72].

With higher SSP concentrations in mixtures, portlandite and the phases resembling C–S–H become more noticeable. However, excessive incorporation of SSP (15%) resulted in a lack of $SiO_2$ and water, with an excess of CaO. Therefore, the SSP-based FSC's high $Ca(OH)_2$ intensity, displayed in Fig. 28A, is responsible for its better mechanical strength over the control FSC, and it is consistent with the results of compressive strength, and the findings of Oyebisi et al. [85]. In addition, the main factor causing the rise of calcium oxide (CaO) levels in SSP-based FSC is the presence of SSP within the cement, given that CaO constitutes the majority of SSP.

From Fig. 28B, the increasing substitution of SSP decreases the formation of calcite ($CaCO_3$), with the lowest peak noticed in mixes containing 15% SSP (15SSP+50GW). According to Abouelnour et al. [55], the partial carbonation of the portlandite caused its levels to decrease when compared to the control FSC.

### 3.3.8. Thermogravimetric analysis (TGA)

In order to assess the behavior of the FSC mixtures at various temperatures, particularly to identify the various crystalline phases present in the sample, a derived thermogravimetric analysis (TGA) and differential thermal analysis (DTA) were suggested in this study. Fig. 29 shows the TGA/DTA curves of the control FSC, 5SSP+50CGW, 10SSP+50GW, and 15SSP+50GGW mixtures after 90

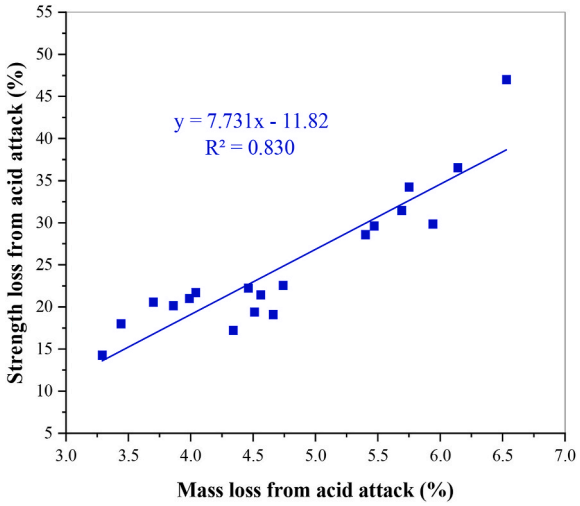



**Fig. 27.** Correlation between mass loss and strength loss of FSC mixtures after acid attack.

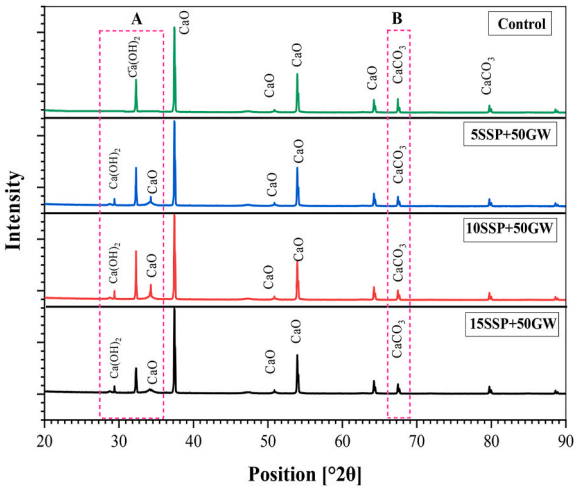



**Fig. 28.** XRD diffractogram of control FSC and mixes with 50% GW and 5, 10, and 15% SSP.

days of hardening. According to the ASTM C1872 standard [86] and the derivative thermogravimetric analysis (TGA) curves (Fig. 29), there are three primary phases in cement hydration products. The first stage is at 100–400 °C, where the dehydration reaction of C–S–H takes place. The second is between 400 and 600 °C which caused by the dehydroxydation of portlandite. The last is between 600 and 1000 °C, representing the decarbonation of $CaCO_3$ [87,88]. It was shown from Fig. 29 that the shape of the TGA curves of the control FSC mixture and mixtures with 50% GW and different SSP contents is essentially comparable, suggesting that the reaction products are essentially identical. The mass losses discovered at 100 °C are associated with the evaporation of free water [57,89]. At 150 °C, about 15% of the concrete's total weight was lost for all tested FSC, which may be associated with the combined water loss of the C–S–H and CH phases [90,91]. Similarly, Yang and Jang [92] detected noticeable weight losses in the DTG test between 0 and 150 °C when replacing 5%, 10%, 15%, and 20% of cement by seashells in alkali-activated slag. They were linked this to the decomposition of the cementitious materials primary hydration products, particularly C–S–H gels. The cement gel compounds (C–S–H and CASH) oxygen bond was broken. The four FSC mixtures tested have an obvious weight loss between 150 and 400 °C which may be associated with the calcium hydroxide phase's water loss. Nevertheless, a remarkable difference between masse losses of 15% SSP based FSC and the other mixtures from 150 °C to 400 °C. Resulting in a decrease in mixture mass at 300 °C by 20% for control FSC and FSC with 5% SSP, 21% for FSC with 10% SSP, and 23% for FSC with 15% SSP. The main reason is that seashell powder increases, with lower activity than cement. The active silicate involved in the hydration reaction decreases, the hydration product decreases, and the weight loss rate increases, which is consistent with the results of DRX analyses and compressive strength. The weight of all FSC mixtures decreases dramatically by 28% as the temperature rises from 400 to 500 °C due portlandite's appearance, which leads to the decomposition of sample, and is in agreement with the finding of Tayeh et al. [10]. Furthermore, a slight variation in weight loss was discovered between 500 and 600 °C for all FSC mixtures, which is in line with the results of Tayeh et al. [10]. Beyond 600 °C, FSC with 10 and 15% SSP showed a weight loss of minus 30% compared to the control mixture and 5%-based FSC. The percentage of weight loss increased

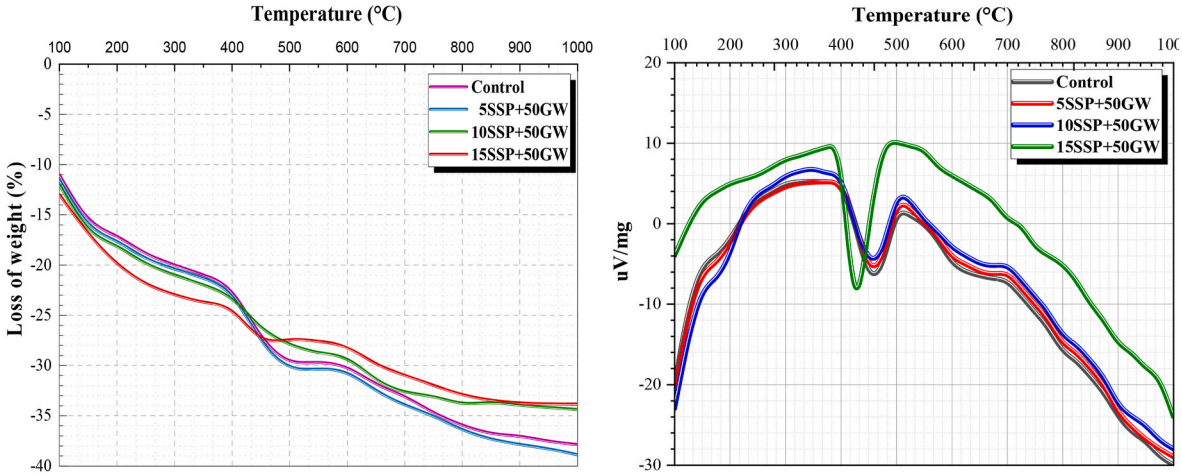



**Fig. 29.** TGA/TDA curves of control FSC and mixes with 50% GW and 5, 10, and 15% SSP.

steadily due to increasing the temperature rates to reach up to 43.3% for control FSC and FSC with 5% SSP, and 35% for FSC with 10 and 15% SSP at 1000 °C. Similarly, Hamada et al. [80] found a weight loss exceeds more than 40% for seashell based concrete at temperature ranging between 670 °C and 800 °C, due to the complete decomposition of carbonates [93]. This finding further supports the results of the XRD tests and is in line with the results of Gong et al. [60], Felipe-Sese et al. [94], and Wang et al. [95], by suggesting that the calcite in the SSP can take part in the hydration process of cements at an early stage. This indicates that, in addition to the compounds resulting from the primary hydration reaction as shown in the XRD analyses (Fig. 28), seashell powder contributes to the chemical reactions those results in the formation of calcite ($CaCO_3$) and to the accumulation of portlandite (CH).

### 3.3.9. SEM analysis

The microscopic morphology can reflect the density, pores size, and cracks width of the concrete mixture. SEM analysis is used in this study to visualize the microstructure development of some FSC samples. In Fig. 30, the SEM images after 90 days of hardening of the 5SSP+50CGW, 10SSP+50GW, and 15SSP+50GGW mixtures are shown.

As it can be seen from Fig. 30, a dense microstructure due to the self-consolidation performance was observed for all mixtures, and may justify the strength development of the studied FSCs. In addition, the incorporation of up to 10% SSP resulted in a reduction in the

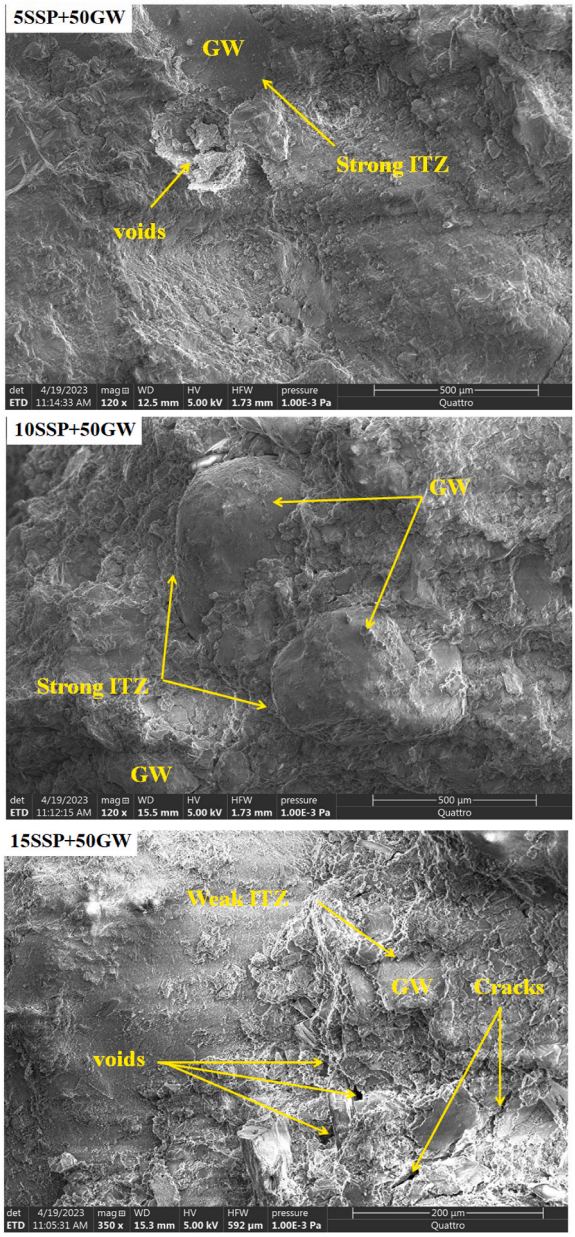



**Fig. 30.** SEM images of control FSC and mixes with 50% GW and 5, 10, and 15% SSP.

void ratio, which validate the results found by the porosity test and supports the increase in strength for these FSC mixtures. Beyond 10% of SSP, the rise in seashell was accompanied by an increase in voids as revealed in Fig. 30. However, the mixtures with 5SSP+50GW and 10SSP+50GW have a denser and continuous structure, with a strong interfacial transition zone (ITZ) between the aggregates and the cement paste, compared to the 15SSP+50GW mixture with a weaker ITZ and more micropores and micro-cracks. Similarly, Maglad et al. [25] found that adding more SSP to lightweight alkali-activated foamed concrete (LFC) increased its void level and therefore weakened the SSP bond mixture. Nonetheless, 10% SSP and 50% GW showed the denser and compact FSC with the fewest voids and cracks, which explains its higher compressive strength than other FSC mixtures. This can be attributed to the filling effect generated by the addition of 5% and 10% SSP [79].

At high levels of cement replacement (15% SSP), some cracks and voids were larger because the SSP used in this study has a high specific surface area, with low activity compared to the cement, which declined the amount of water to clinker content, and the amount of hydration products produced. The water content of the adsorbed layer in the system rises and the free water content falls when the amount of SSP is too high [96]. According to Othman et al. [78], Wang et al. [88], and Liu et al. [97], the large specific surface area of SSP can fill the pores with C–S–H gel, and decreased the overall porosity. However, with higher cement replacement rate, the generated C–S–H gel was unable to fill more micro-pores, which decreased the secondary hydration degree and raised the overall porosity [97]. Partial gel was occurred on the aggregates surface and no gel material was found for filling and bonding between the aggregates and the matrix. However, there are limitations on the bond between the aggregate and paste, as well as the compactness of the mixing matrix. As a result, this event will weaken the inner part's cement paste-aggregate link and consistent with another study that found that adding more oyster shell powder raised the amount of voids in geopolymer concrete [9,92]. Stel'makh et al. [98] also showed more integral microstructure without voids and cracks by adding 6% SSP to concrete. However, the fine pores have become a little larger when 30% of SSP was added. In addition, the effect of GW on the microstructure of FSC could be observed in Fig. 30. It is important to note from this figure, that for all FSC mixtures based on 50% GW, a strong ITZ between GW grains and cement paste was observed, which corresponds to the high compressive strength and consistent with the previous studies reported [55,56,99,100].

### 3.4. Environmental impact assessment

Environmental impact assessment is useful to provide information about the environmental pollutants and nonrenewable raw materials consumption. As well as, identify the energy efficiency and suggest improvement criteria [101]. In recent years, the evaluation of concrete production impacts on the increase in $CO_2$ emissions and the consumption of non-renewable resources is very important [102]. In this study, the environmental impact assessment for one cubic meter FSC mixes was determined to show that the developed FSCs are effective and eco-friendly products. It is estimated based on the amount of $CO_2$ emissions and the volume of raw materials (RM) consumption for each FSC mixture. The volume of RM consumption (cement and natural river sand) is calculated based on the material proportion for each FSC mix described in Table 3. The quantity of $CO_2$ emissions is calculated based on the value of $CO_2$ emitted by the cement of 1.77 kg $CO_2$/kg and 0.37 kg $CO_2$/kg for natural sand, according to the results of Sudjono and Yudhi [50]. The results of RM consumption volume and $CO_2$ emission quantity for all FSC mixes are presented in Figs. 31 and 32, respectively. It can be seen from these figures that the volume of RM consumption and the amount of $CO_2$ emissions decrease linearly with the increase of SSP and GW by partially replacing cement and natural river sand, respectively. The highest volume of RM consumption and the highest quantity of $CO_2$ emissions were found with the control FSC, and the lowest ones were observed for the mixture with a high content of recycled waste (15SSP + 50GW). It can be seen from these results that the best environmental impact was found when 15 wt% SSP and 50 vol% GW were added, with 873.94 kg/m$^3$ of $CO_2$ emissions and 68.25% of RM consumption. These values are reduced by 31.75% and 29.11%, respectively, for control FSC with 100% RM and 1232.83 kg/m$^3$ $CO_2$ emissions. Similarly, Ahmadi et al. [66] showed a decrease of about 16.4 and 32.4%, in RM consumption and $CO_2$ emissions, respectively, by partially replacing the sand with granite waste. De Schepper et al. [103] also reported that using recycled aggregate with ordinary strength concrete reduces the $CO_2$ emissions

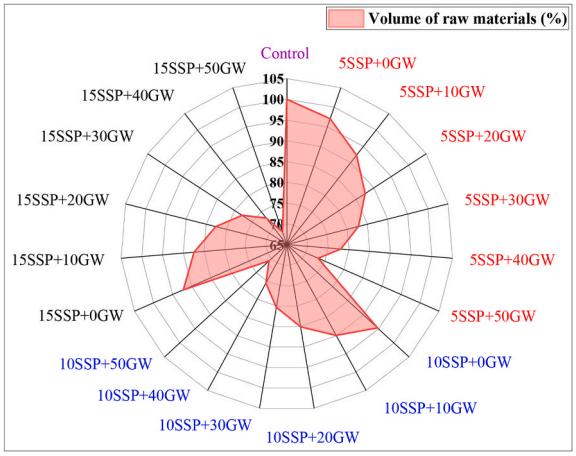



**Fig. 31.** Environmental impact by volume of raw materials consumption for all FSC mixture.

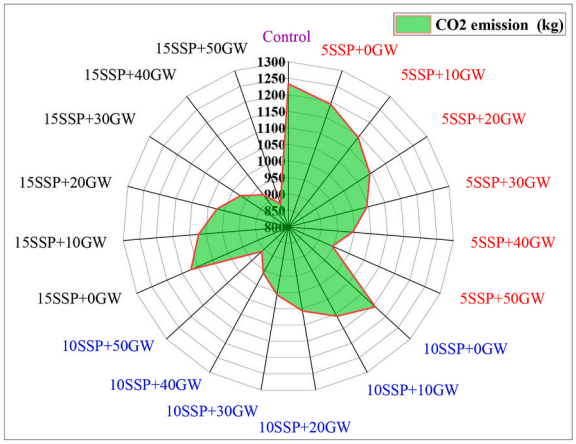



**Fig. 32.** Environmental impact by $CO_2$ emission of all FSC mixture.

by 35%. Moreover, Guo et al. [104] found approximately 16.1% reduction in the negative environmental impact compared to ordinary concrete by using recycled aggregates.

Finally, this result could prove that the synergistic use of SSP as cement and GW as sand in FSC production benefits the environmental impact and waste consumption by reducing $CO_2$ emissions and natural resource consumption. Since SSP and GW all belong to solid waste, they bring high value-added benefits both economically and environmentally.

## 4. Conclusion

The present study examine + d the simultaneous utilization of SSP as a supplementary cementitious addition and GW as fine aggregates in developing sustainable flowable sand concrete. Based on the obtained experimental results, the following conclusion could be drawn.

- Using up to 50% GW as a partial replacement of fine aggregate decreases the flow of FSC; but it remains within the acceptable limit prescribed by the EFNARC recommendations. However, with a low dosage of superplasticizer, the addition of SSP as filler compensates for the negative effect of GW and improves the fresh properties (slump flow and V-funnel flow time) of FSC mixtures.
- For all curing ages, the compressive strength increases as the quantity of GW in FSC increases. However, the presence of SSP enhances the compressive strength of the GW-based mixtures better than that of the control FSC. The combined use of 10% SSP and 50% GW increased the compressive strength of control FSC by 66.40% at 90 days, developing high-strength FSC with 66.51 MPa.
- The UPV and modulus of elasticity of the FSC mixture increase with the increasing substitution of natural sand by GW. However, 10% SSP-based FSC mixes exhibit the highest values, which increased from 3830 m/s and 33.15 GPa for control FSC to 4172 m/s and 40.16 GPa for the mixture with 10% SSP and 50% GW.
- The porosity and water absorption of FSC decreased with the combined use of SSP and GW. Mixtures with 10% SSP and 50% GW exhibited the weakest values, with approximately 45.06% and 6.33% decreases in porosity and water absorption, respectively, compared to the control FSC.
- The durability of FSC with SSP and GW against acid attack is higher than that of the control FSC, which can be adapted to aggressive environments.
- The XRD, TGA, and SEM analyses revealed that using up to 10% SSP and 50% GW gave denser microstructure, less porosity, and stronger ITZ between cement paste and aggregates of FSC mixtures compared to control FSC.
- The synergistic use of SSP as cement and GW as sand in FSC production benefits the environmental impact and waste consumption by reducing $CO_2$ emissions and natural resource consumption.

Based on the outcomes, fresh and hardened characteristics, durability indexes, microstructural analyses, and environmental impact assessment. It can be concluded that the combined use of up to 50% of GW as fine aggregate and 10% of SSP as cement in FSC is highly recommended since their addition not only contributes to solving environmental problems by reducing the level of waste, $CO_2$ emissions, and the extraction of natural resources, but would also enhance the physical and mechanical performance of FSC. All the studied FSC mixes are considered satisfactory for the application of structural elements.

## CRediT authorship contribution statement

**Moussa Hadjadj:** Writing – original draft, Formal analysis, Data curation, Conceptualization. **Mohamed Guendouz:** Visualization, Validation, Supervision, Methodology. **Djamila Boukhelkhal:** Writing – review & editing, Resources, Project administration.

## Declaration of competing interest

The authors declare that they have no known competing financial interests or personal relationships that could have appeared to influence the work reported in this paper.

## Data availability

No data was used for the research described in the article.

## Acknowledgment

The authors would like to thank all persons who helped them throughout the research, particularly the personnel of Civil Engineering Laboratory of the University of Medea.

## References

[1] M. Guendouz, Dj Boukhelkhal, Properties of flowable sand concrete containing ceramic wastes, J. Adhes. Sci. Techn. 33 (24) (2019) 2661–2683.
[2] W. Cui, W.S. Yan, H.F. Song, X.L. Wu, Blocking analysis of fresh self-compacting concrete based on the DEM, Constr. Build. Mater. 168 (2018) 412–421.
[3] M. Guendouz, Dj Boukhelkhal, A. Bourdot, Recycling of floor tile waste as fine aggregate in flowable sand concrete, in: Adva. Gre. Energ. Mater. Techn, Springer, 2021, pp. 223–229.
[4] Dj Boukhelkhal, O. Boukendakdji, S. Kenai, E.H. Kadri, Combined effect of mineral admixture and curing temperature on mechanical behavior and porosity of SCC, Adv. Concret. Constr. 6 (1) (2018) 69–85, https://doi.org/10.12989/acc.2018.6.1.069.
[5] Y.F. Silva, D.A. Lange, S. Delvasto, Effect of incorporation of masonry residue on the properties of self-compacting concretes, Constr. and Build. Mater. 196 (2019) 277–283.
[6] M. Guendouz, Dj Boukhelkhal, A. Mechantel, T. Boukerma, Valorization of coffee waste as bio-aggregates in crushed sand concrete production, Envir. Engineer. Manag. J. 22 (1) (2023) 147–156, https://doi.org/10.30638/eemj.2023.013.
[7] H. Blaifi, M. Guendouz, A.E. Belhadj, Dj Boukhelkhal, M. Hadjadj, Sustainable use of recycled plastic and ceramic industrial wastes in eco-friendly construction materials, Envir. Engineer. Manag. J. 22 (8) (2023) 1479–1494. http://www.eemj.icpm.tuiasi.ro/. http://www.eemj.eu.
[8] G.O. Bamigboye, O. Okara, D.E. Bassey, K.J. Jolayemi, D. Ajimalofin, The use of *Senilia senilis* seashells as a substitute for coarse aggregate in eco-friendly concrete, J. Build. Eng. 32 (2020) 101811, https://doi.org/10.1016/j.jobe.2020.101811.
[9] W. Okoro, S. Oyebisi, Mechanical and durability assessments of steel slag-seashell powder-based geopolymer concrete, Heliyon 9 (2023) e13188, https://doi.org/10.1016/j.heliyon.2023.e13188.
[10] B.A. Tayeh, M.W. Hasaniyah, A.M. Zeyad, M.M. Awad, A. Alaskar, A.M. Mohamed, R. Alyousef, Durability and mechanical properties of seashell partially-replaced cement, J. Build. Eng. 31 (2020) 101328, https://doi.org/10.1016/j.jobe.2020.101328.
[11] C. Punthama, N. Supakata, V. Kanokkantapong, Characteristics of concrete bricks after partially substituting Portland cement type 1 with cement and seashell waste and partially substituting sand with Glass waste, Environment Asia 12 (1) (2019).
[12] S. Kavitha, T.F. Kala, Evaluation of strength behavior of self-compacting concrete using alccofine and GGBS as partial replacement of cement, Ind. J. Sci. Techn. 9 (22) (2016) 1–5.
[13] K.H. Mo, U.J. Alengaram, M.Z. Jumaat, S.C. Lee, W.I. Goh, C.W. Yuen, Recycling of seashell waste in concrete: a review, Constr. Build. Mater. 162 (2018) 751–764, https://doi.org/10.1016/j.conbuildmat.2017.12.009.
[14] B. Chen, L. Peng, H. Zhong, Y. Zhao, T. Meng, B. Zhang, Synergetic recycling of recycled concrete aggregate and waste mussel shell in concrete: mechanical properties, durability and microstructure, Construct. Build. Mater. 371 (2023) 130825, https://doi.org/10.1016/j.conbuildmat.2023.130825.
[15] B. Zhong, Q.Z.C. Chan, Y. Yu, Structure and property characterization of oyster shell cementing material, Chin. J. Struct. Chem. 31 (1) (2012) 85–92.
[16] P. Lertwattanaruk, N. Makul, C. Siripattarapravat, Utilization of ground waste seashells in cement mortars for masonry and plastering, J. Envir. Manag. 111 (2012) 133–141.
[17] G.O. Bamigboye, A.T. Nworgu, A.O. Odetoyan, M. Kareem, D.O. Enabulele, D.E. Bassey, Sustainable use of seashells as binder in concrete production: Prospect and challenges, J. Build. Eng. 34 (2021) 101864, https://doi.org/10.1016/j.jobe.2020.101864.
[18] E. Khankhaje, T. Kim, H. Jang, M. Rafieizonooz, Laboratory evaluation of heavy metal removal from stormwater runoff by pervious concrete pavement containing seashell and oil palm kernel shell, Construct. Build. Mater. 400 (2023) 132648, https://doi.org/10.1016/j.conbuildmat.2023.132648.
[19] C. Martínez-García, B. Gonzalez-Fonteboa, D. Carro-Lopez, F. Martínez-Abella, Mussel shell mortars durability: study of aggregate replacement limit, J. Build. Eng. 82 (2024) 108239, https://doi.org/10.1016/j.jobe.2023.108239.
[20] M.H. Ahsan, M.S. Siddique, S.H. Farooq, M. Usman, M.A.U. Aleem, M. Hussaina, A. Hanif, Mechanical behavior of high-strength concrete incorporating seashell powder at elevated temperatures, J. Build. Eng. 50 (2022) 104226, https://doi.org/10.1016/j.jobe.2022.104226.
[21] J.H. Seo, S.M. Park, B.J. Yang, J.G. Jang, Calcined oyster shell powder as an expansive additive in cement mortar, Materials 12 (8) (2019) 1322.
[22] A. Abdelouahed, et al., Effect of cockele shells on mortars performance in extreme conditions, Civil and Envir. Engin. Repor. 29 (2) (2019) 60–73.
[23] C.R. Rollakanti, et al., An experimental investigation on mechanical properties of concrete by partial replacement of cement with wood ash and fine sea shell powder, Mater. Tod. Proceedings 43 (2021) 1325–1330.
[24] F. Soltanzadeh, et al., Development and characterization of blended cements containing seashell powder, Constr. Build. Mater. 161 (2018) 292–304, https://doi.org/10.1016/j.conbuildmat.2017.11.111.
[25] A.M. Maglad, M.A.O. Mydin, S.D. Datta, B.A. Tayeh, Assessing the mechanical, durability, thermal and microstructural properties of sea shell ash based lightweight foamed concrete, Construct. Build. Mater. 402 (2023) 133018, https://doi.org/10.1016/j.conbuildmat.2023.133018.
[26] P. Sangeetha, M. Shanmugapriya, K.S. Saravanan, P. Prabhakaran, V. Shashankar, Mechanical properties of concrete with seashell waste as partial replacement of cement and aggregate, Mater. Today: Proc. 61 (2022) 320–326, https://doi.org/10.1016/j.matpr.2021.09.501.
[27] C. Wei, X. Liu, Z. Zhang, P. Wu, Utilization of solid wastes for aerated concrete preparation: mechanical properties and microstructural analysis, J. Build. Eng. 82 (2024) 108235, https://doi.org/10.1016/j.jobe.2023.108235.
[28] A. Jain, R. Gupta, S. Chaudhary, Sustainable development of self-compacting concrete by using granite waste and fly ash, Constr. Build. Mater. 262 (2020) 120516.
[29] S. Kumar, A.K. Mishra, Influence of granite fine powder on the performance of cellular light weight concrete, J. Build. Eng. 40 (2021) 102707, https://doi.org/10.1016/j.jobe.2021.102707.
[30] M.A. Rashwan, T.M. Al-Basiony, A.O. Mashaly, M.M. Khalil, Behaviour of fresh and hardened concrete incorporating marble and granite sludge as cement replacement, J. Build. Eng. 32 (2020) 101697, https://doi.org/10.1016/j.jobe.2020.101697.
[31] S.K. Nayak, A. Satapathy, S. Mantry, Use of waste marble and granite dust in structural applications: a Review, J. Build. Eng. 46 (2022) 103742, https://doi.org/10.1016/j.jobe.2021.103742.
[32] A. Karmegam, A. Kalidass, D. Ulaganathan, Utilization of granite sawing waste in self compacting concrete, Journal of the Croatian Association of Civil Engineers 66 (11) (2014) 997–1006.

[33] S. Singh, R. Nagar, V. Agrawal, Feasibility as a potential substitute for natural sand: a comparative study between granite cutting waste and marble slurry, Proced. Envir. Sci. 35 (2016) 571–582.
[34] M. Vijayalakshmi, A.S.S. Sekar, Strength and durability properties of concrete made with granite industry waste, Construct, Build. Mater. 46 (2013) 1–7, https://doi.org/10.1016/j.conbuildmat.2013.04.018.
[35] S. Ghannam, H. Najm, R. Vasconez, Experimental study of concrete made with granite and iron powders as partial replacement of sand, Sust. Mater. Techn. 9 (2016) 1–9.
[36] G.C. Cordeiro, L.M.S.C. de Alvarenga, C.A.A. Rocha, Rheological and mechanical properties of concrete containing crushed granite fine aggregate, Constr. Build. Mater. 111 (2016) 766–773.
[37] H. Binici, O. Aksogan, Durability of concrete made with natural granular granite, silica sand and powders of waste marble and basalt as fine aggregate, J. Build. Eng. 19 (2018) 109–121, https://doi.org/10.1016/j.jobe.2018.04.022.
[38] P. Nuaklong, P. Worawatnalunart, P. Jongvivatsakul, S. Tangaramvong, T. Pothisiri, S. Likitlersuang, Pre- and post-fire mechanical performances of high calcium fly ash geopolymer concrete containing granite waste, J. Build. Eng. 44 (2021) 103265, https://doi.org/10.1016/j.jobe.2021.103265.
[39] A. Jain, R. Gupta, S. Gupta, S. Chaudhary, Evaluation of real time fire performance of eco-efficient fly ash blended self-consolidating concrete including granite waste, J. Build. Eng. 77 (2023) 107553, https://doi.org/10.1016/j.jobe.2023.107553.
[40] NF EN, 197-1: 2000, Cement: Part 1: Composition, Specifications and Conformity Criteria for Common Cements", British Standards Institute, 389 Chiswick High Road, London, W4 4AL, 2000.
[41] S. Sablocrete, Concrete: Characteristics and Use Practices, Presses de l'Ecole Nationale des Ponts et Chaussées LCPC, Paris, 1994.
[42] EN EN., 1008, Mixing Water for Concrete - Specifications for Sampling, Testing and Evaluation of Suitability for Use, Including Process Waters of the Concrete Industry, Such as Concrete Mixing Water, AFNOR, 2003.
[43] S. Efnarc, Guidelines for Self-Compacting Concrete, European Federation for Specialist Construction Chemicals and Concrete Systems, English ed., February, 2002. Norfolk, UK.
[44] Dj Boukhelkhal, M. Guendouz, A. Bourdot, H. Cheriet, K. Messaoudi, Elaboration of bio-based building materials made from recycled olive core, MRS Energy & Sustainab. 8 (2021) 98–109, https://doi.org/10.1557/s43581-021-00006-8.
[45] NF EN 196-1, Methods of Testing Cement—Part 1: Determination of Strength. Turkish Standards Institution, 2002, AFNOR.
[46] ASTM C469/C469M-14Standard Test Method for Static Modulus of Elasticity and Poisson's Ratio of Concrete in Compression, 2014.
[47] ASTM C567-16, Standard Test Method for Pulse Velocity through Concrete, ASTM International, West Conshohocken, PA, 2009, 597.
[48] ASTM C642, Standard Test Method for Density, Absorption, and Voids in Hardened Concrete, ASTM, ASTM International, 2013.
[49] ASTM C307-03, in: Standard Test Method for Tensile Strength of Chemical-Resistant Mortar, Grouts and Monolithic Surfacing, ASTM International, West Conshohocken, PA, USA, 2012. Committee C-1 on Cement.
[50] P. Sudjono, C.O. Yudhi, Estimasi Emisi CO2 Dari Pembangunan Berbagai Ukuran Rumah Sederhana, Jurnal Teknik Lingkungan 17 (2) (2011) 98–109.
[51] R.H. Suwarno, A.S. Yuwono, On the performance analysis and environmental impact of concrete with coal fly ash and Bottom ash, International Journal of Engineering & Technology Innovation 13 (1) (2023).
[52] EN 1097-6, Tests for Mechanical and Physical Properties of Aggregates - Part 6: Determination of Particle Density and Water Absorption, AFNOR, 2022.
[53] K. Yamaguchi, S. Hashimoto, Cold sintering of calcium carbonate derived from seashells, Open Ceramics 12 (2022) 100302, https://doi.org/10.1016/j.oceram.2022.100302.
[54] A. Jain, R. Gupta, S. Chaudhary, Performance of self-compacting concrete comprising granite cutting waste as fine aggregate, Construct. Build. Mater. 221 (2019) 539–552, https://doi.org/10.1016/j.conbuildmat.2019.06.104.
[55] M.A. Abouelnour, M.A. Abd EL-Aziz, K.M. Osman, I.N. Fathy, B.A. Tayeh, M.E. Elfakharany, Recycling of marble and granite waste in concrete by incorporating nano alumina, Construct. Build. Mater. 411 (2024) 134456, https://doi.org/10.1016/j.conbuildmat.2023.134456.
[56] A. Karimipour, H. Jahangir, D.R. Eidgahee, A thorough study on the effect of red mud, granite, limestone and marble slurry powder on the strengths of steel fibres-reinforced self-consolidation concrete: experimental and numerical prediction, J. Build. Eng. 44 (2021) 103398, https://doi.org/10.1016/j.jobe.2021.103398.
[57] G. Lin, L. Zhang, P. Cheng, X. Yu, C. Miao, K. Qian, S. Ruan, X. Qian, Application potential of granite cutting waste and tunnel excavation rock as fine aggregates in cement-based materials based on surface characteristics, J. Build. Eng. 62 (2022) 105380, https://doi.org/10.1016/j.jobe.2022.105380.
[58] M. Mageswari, et al., To increase the strength of concrete by adding seashell as admixture, Inter. J. Adv. Resea. Civil, Struct., Envir. Infr. Eng. Devel. 2 (2) (2016) 165–174.
[59] J. Wang, E. Liu, Upcycling waste seashells with cement: Rheology and early-age properties of Portland cement paste, Res. Conser. Recy. 155 (2020) 104680, https://doi.org/10.1016/j.resconrec.2020.104680.
[60] Y. Gong, C. Shao, Z. Wang, R. Liu, Q. Zhang, Z. Ren, Z. Zhu, D. Zhao, J. Bai, J. Tian, M. Chen, Feasibility study on the preparation of ternary cement with calcined slag powder and seashell powder as supplementary cementitious materials, Construct. Build. Mater. 409 (2023) 134223, https://doi.org/10.1016/j.conbuildmat.2023.134223.
[61] K. Hasan, et al., Investigation on the properties of mortar containing palm oil fuel ash and seashell powder as partial cement replacement, Constr. Met. (CTICM) 1 (2) (2021) 50–61.
[62] M. Olivia, R. Oktaviani, Properties of concrete containing ground waste cockle and clam seashells, Proc. Eng. 171 (2017) 658–663.
[63] G. Li, et al., Properties of cement-based bricks with oyster-shells ash, J. Clean. Produc. 91 (2015) 279–287.
[64] P.H. Borges, et al., Carbonation of CH and C–S–H in composite cement pastes containing high amounts of BFS, Cem. concr. resear. 40 (2) (2010) 284–292.
[65] R. Yang, R. Yu, Z.H. Shui, C. Guo, S. Wu, X. Gao, S. Peng, The physical and chemical impact of manufactured sand as a partial replacement material in Ultra-High Performance Concrete (UHPC), Cement Concr. Compos. 99 (2019) 203–213.
[66] S.F. Ahmadi, M. Reisi, M.C. Amiri, Reusing granite waste in eco-friendly foamed concrete as aggregate, J. Build. Eng. 46 (2022) 103566, https://doi.org/10.1016/j.jobe.2021.103566.
[67] M.V.S. Reddy, et al., Durability aspects of standard concrete, Inter. J. Struc. Civ. Engin. Resea. 2 (1) (2013) 40–46.
[68] Dj Boukhelkhal, M. Guendouz, The use of non-destructive tests to estimate Self-compacting concrete compressive strength, MATEC Web of Conferences 149 (2018) 01036.
[69] T.R. Naik, V.M. Malhotra, J.S. Popovics, The Ultrasonic Pulse Velocity Method, Handbook on Nondestructive Testing of Concrete, CRC Press LLC, 2004.
[70] B. Wu, H. Cao, Q. Wu, Compressive and shrinkage behaviors of recycled aggregate concrete containing recycled sand from weathered residual soil of granite and MgO expansion agent, J. Build. Eng. 68 (2023) 106154, https://doi.org/10.1016/j.jobe.2023.106154.
[71] M. Olivia, A.A. Mifshella, L. Darmayanti, Mechanical properties of seashell concrete, Procedia Eng. 125 (2015) 760–764.
[72] B.A. Tayeh, M.W. Hasaniyah, A. Zeyad, M.O. Yusuf, Properties of concrete containing recycled seashells as cement partial replacement: a review, J. Clean. Prod. 237 (2019) 117723.
[73] C. Pellegrino, Y. Gaddo, Mechanical and durability characteristics of concrete containing EAF slag as aggregate, Cement Concr. Compos. 31 (2009) 663–671, https://doi.org/10.1016/J.CEMCONCOMP.2009.05.006.
[74] R. Hay, B. Peng, K. Celik, Filler effects of CaCO3 polymorphs derived from limestone and seashell on hydration and carbonation of reactive magnesium oxide (MgO) cement (RMC), Cem. Concr. Resea. 164 (2023) 107040, https://doi.org/10.1016/j.cemconres.2022.107040.
[75] Y. Liu, B. Wang, Z. Liu, Y. Zou, Y. Teng, Y. Ji, Sustainable utilization of waste oyster shell powders with different fineness levels in a ternary supplementary cementitious material system, Sustainability 14 (2022) 5981.
[76] A. Jain, et al., Abrasion resistance and sorptivity characteristics of SCC containing granite waste, Mater. Toda. Proc. 27 (2020) 524–528.
[77] H.M. Hamada, F. Abed, B. Tayeh, M.S.Al Jawahery, A. Majdi, S.T. Yousif, Effect of recycled seashelles on concrete properties: A comprehensivereview of the recent studies, Constr. Bluid. Mater. 376 (2023), https://doi.org/10.1016/j.conbuildmat.2023.131036.
[78] N.H. Othman, et al., Cockle shell ash replacement for cement and filler in concrete, Malay. J. Civ. Eng. 25 (2) (2013) 201–211.

[79] Y. Liao, et al., Effect of waste oyster shell powder content on properties of cement-metakaolin mortar, Case Stud. Constr. Mater. 16 (2022) 01088.
[80] S. Singh, R. Nagar, V. Agrawal, Performance of granite cutting waste concrete under adverse exposure conditions, J. Clean. Prod. 127 (2016) 172, https://doi.org/10.1016/j.jclepro.2016.04.034.
[81] D. Das, P.K. Rout, Synthesis of Inorganic Polymeric materials from industrial solid waste, Silicon 15 (2023) 1771–1791, https://doi.org/10.1007/s12633-022-02116-5.
[82] S. Ghorbani, I. Taji, J. De Brito, M. Negahban, S. Ghorbani, M. Tavakkolizadeh, A. Davoodi, Mechanical and durability behaviour of concrete with granite waste dust as partial cement replacement under adverse exposure conditions, Constr. Build. Mater. 194 (2019) 143–152.
[83] A. Qasem, M. Almekhlafi, F. Yahaya, The effect of palm oil fuel clinker powder and cockleshell powder as cement replacement on durability properties of the concrete mortar, in: IOP Conference Series: Earth and Envir. Sci., IOP Publishing, 2021.
[84] S. Oyebisi, A. Ede, F. Olutoge, D. Omole, Geopolymer concrete incorporating agro-industrial wastes : effects on mechanical properties , microstructural behaviour and mineralogical phases, Construct. Build. Mater. 256 (2020) 119390, https://doi.org/10.1016/j.conbuildmat.2020.119390.
[85] S. Oyebisi, A. Ede, F. Olutoge, D. Olukanni, Assessment of activity moduli and acidic resistance of slag-based geopolymer concrete incorporating pozzolan, Case Stud. Constr. Mater. 13 (2020) e00394, https://doi.org/10.1016/j.cscm.2020.e00394.
[86] ASTM C1872, Standard Test Method for Thermogravimetric Analysis of Hydraulic Cement, ASTM, ASTM International, 2018.
[87] V. Hallet, M.T. Pedersen, B. Lothenbach, F. Winnefeld, N. De Belie, Y. Pontikes, Hydration of blended cement with high volume iron-rich slag from non-ferrous metallurgy, Cem. Concr. Res. 151 (2022).
[88] J. Wang, E. Liu, L. Li, Characterization on the recycling of waste seashells with Portland cement towards sustainable cementitious materials, J. Clean. Prod. 220 (2019) 235–252.
[89] W. Deboucha, N. Leklou, A. Khelidj, M.N. Oudjit, Hydration development of mineral additives blended cement using thermogravimetric analysis (TGA): Methodology of calculating the degree of hydration, Construct. Build. Mater. 146 (2017) 687–701.
[90] J. Wang, E. Liu, Upcycling waste seashells with cement: Rheology and early-age properties of Portland cement paste, Resour. Conserv. Recycl. 155 (2020) 104680.
[91] Y. Wei, W. Yao, X. Xing, M. Wu, Quantitative evaluation of hydrated cement modified by silica fume using QXRD, 27Al MAS NMR, TG–DSC and selective dissolution techniques, Constr. Build. Mater. 36 (2012) 925–932.
[92] B. Yang, J.G. Jang, Environmentally benign production of one-part alkali-activated slag with calcined oyster shell as an activator, Constr. Build. Mater. 257 (2020) 119552, https://doi.org/10.1016/j.conbuildmat.2020.119552.
[93] B. Safi, M. Saidi, A. Daoui, A. Bellal, A. Mechekak, K. Toumi, The use of seashells as a fine aggregate (by sand substitution) in self-compacting mortar (SCM), Constr. Build. Mater. 78 (2015) 430–438.
[94] M. Felipe-Ses'e, D. Eliche-Quesada, F. Corpas-Iglesias, The use of solid residues derived from different industrial activities to obtain calcium silicates for use as insulating construction materials, Ceram. Int. 37 (2011) 3019–3028.
[95] H. Wang, P.K. Hou, Q.F. Li, S. Adu-Amankwah, H. Chen, N. Xie, P.Q. Zhao, Y.B. Huang, S.D. Wang, X. Cheng, Synergistic effects of supplementary cementitious materials in limestone and calcined clay-replaced slag cement, Constr. Build. Mater. 282 (2021) 12.
[96] C. Chandrasiri, T. Yehdego, S. Peethamparan, Synthesis and characterization of bio-cement from conch shell waste, Constr. Build. Mater. 212 (2019) 775–786.
[97] S. Liu, Y. Zhang, B. Liu, Z. Zou, Q. Liu, Y. Teng, L.V. Zhang, Sustainable use of waste oyster shell powders in a ternary supplementary cementitious material system for green concrete, Materials 15 (14) (2022) 4886.
[98] S.A. Stel'makh, E.M. Shcherban, A.N. Beskopylny, L.R. Mailyan, B. Meskhi, S.Sh Tashpulatov, A. Chernil'nik, N. Shcherban, A. Tyutina, Composition, Technological, and microstructural aspects of concrete modified with finely ground mussel shell powder, Materials 16 (1) (2023) 82, https://doi.org/10.3390/ma16010082.
[99] W.L. Zhang, Zai-JianYuan, D.Q. Li, Y.S. Liao, L.Y. Zhao, Application potentials of decomposed granite from Benggang area in South China as fine aggregates in cement-based materials, Construct. Build. Mater. 310 (2021) 125109.
[100] S. Tangaramvong, P. Nuaklong, M.T. Khine, P. Jongvivatsakul, The influences of granite industry waste on concrete properties with different strength grades, Case Stud. Constr. Mater. 15 (2021) e00669, https://doi.org/10.1016/j.cscm.2021.e00669.
[101] I.O.f. Standardization, Environmental Management: Life Cycle Assessment; Principles and Framework, ISO, 2006.
[102] S. Ross, D. Evans, M. Webber, How LCA studies deal with uncertainty, Int. J. Life Cycle Assess. 7 (1) (2002) 47–52.
[103] M. De Schepper, P. Van den Heed, I. Van Driessche, N.De Belie, Life cycle assesment of completely recyclable concrete, Materials 7 (8) 201460106027.
[104] Z. Guo, A. Tu, C. Chen, D.E. Lehman, Mechanical properties, durability and life-cycle assesment of concrete building blocks incorporating recycled concrete aggregate, J. Clean. Prod. 199 (2018) 136–149.